JOURNAL OF VIROLOGY, May 2008, p. 4991–5006 Vol. 82, No. 10
0022-538X/08/$08.00+0 doi:10.1128/JVI.02586-07

Triple Gene Block Protein Interactions Involved in Movement of *Barley Stripe Mosaic Virus*▽

Hyoun-Sub Lim,[1,2] Jennifer N. Bragg,[1] Uma Ganesan,[1] Diane M. Lawrence,[1] Jialin Yu,[3] Masimachi Isogai,[1,4] John Hammond,[2] and Andrew O. Jackson[1]*

Department of Plant and Microbial Biology, University of California, Berkeley, California 94720[1]; U.S. Department of Agriculture, FNPRU—Agricultural Research Service, Beltsville, Maryland 20705[2]; State Key Laboratory of Agrobiotechnology, College of Biological Sciences, China Agricultural University, Beijing, China[3]; and Plant Pathology Laboratory, Iwate University, Morioka 020-8550, Japan[4]

Received 4 December 2007/Accepted 29 February 2008

Barley stripe mosaic virus **(BSMV) encodes three movement proteins in an overlapping triple gene block (TGB), but little is known about the physical interactions of these proteins. We have characterized a ribonucleoprotein (RNP) complex consisting of the TGB1 protein and plus-sense BSMV RNAs from infected barley plants and have identified TGB1 complexes in planta and in vitro. Homologous TGB1 binding was disrupted by site-specific mutations in each of the first two N-terminal helicase motifs but not by mutations in two C-terminal helicase motifs. The TGB2 and TGB3 proteins were not detected in the RNP, but affinity chromatography and yeast two-hybrid experiments demonstrated that TGB1 binds to TGB3 and that TGB2 and TGB3 form heterologous interactions. These interactions required the TGB2 glycine 40 and the TGB3 isoleucine 108 residues, and BSMV mutants containing these amino acid substitution were unable to move from cell to cell. Infectivity experiments indicated that TGB1 separated on a different genomic RNA from TGB2 and TGB3 could function in limited cell-to-cell movement but that the rates of movement depended on the levels of expression of the proteins and the contexts in which they are expressed. Moreover, elevated expression of the wild-type TGB3 protein interfered with cell-to-cell movement but movement was not affected by the similar expression of a TGB3 mutant that fails to interact with TGB2. These experiments suggest that BSMV movement requires physical interactions of TGB2 and TGB3 and that substantial deviation from the TGB protein ratios expressed by the wild-type virus compromises movement.**

For a virus to successfully invade a plant and cause disease, it must have the ability to move from cell to cell, establish localized infection foci, enter and exit the vascular system, and develop systemic infections. To accomplish these activities, plant viruses encode one or more movement proteins (MPs) that facilitate cell-to-cell movement and vascular transport. These proteins generally localize at plasmodesmata (PD) and increase the permeability of the PD sufficiently to permit the movement of macromolecules through the desmotubule (25, 38). Many MPs have RNA binding activities, and some act in concert with other virus-encoded proteins to facilitate virus movement and other activities such as RNA unwinding (18) or suppression of gene silencing (1, 24). Several general classes of viral MPs are known to exist, and these proteins provide tools for investigating a wide range of host-virus interactions and cellular functions (25, 26).

The most extensively investigated MPs are members of the 30K superfamily that are encoded by a large number of RNA and DNA viruses with different genome organizations (27). Over the past 15 years, studies of the processes carried out by proteins of the 30K movement family have provided great insight into the requirements for local and long-distance transport of *Tobacco mosaic virus* and a number of other viruses (4, 15, 25, 38). The triple gene block (TGB) superfamily represents another major class of MPs encoded by taxonomically diverse RNA viruses (29). In this superfamily, the three genes required for movement are organized into overlapping open reading frames (ORFs) and function in concert to mediate virus movement. Numerous studies have shown that the molecular properties of the TGB proteins and the 30K MPs are quite distinct, and sequence analyses suggest that they have undergone convergent evolution (27, 29, 39).

The TGB superfamily can be subdivided into two major classes that have substantial differences in structure and in the requirement of the coat protein (CP) for cell-to-cell and vascular movement (29). Class I, or hordeivirus-like, TGB proteins are encoded by tubular viruses consisting of the *Benyvirus*, *Hordeivirus*, *Pecluvirus*, and *Pomovirus* genera, in which the CP is dispensable for cell-to-cell movement (4, 29, 31). Class II, or potexvirus-like, MPs are represented by flexuous viruses that have been classified into the *Allexivirus*, *Carlavirus*, *Foveavirus*, and *Potexvirus* genera, which require the CP for movement (8, 19, 35, 36, 37). Studies focusing on the hordeiviruses, primarily *Barley stripe mosaic virus* (BSMV) and *Poa semilatent virus* (PSLV), and the potexvirus *Potato virus X* (PVX) have clearly shown that the TGB movement strategy requires the coordinated activities of each of the TGB proteins (6, 22, 36) and that their levels of expression are mediated by transcription and translation from two subgenomic RNAs (sgRNAs) (17, 35, 41). However, only limited evidence is available about the physical interactions of the TGB proteins or the importance of these interactions in movement. Therefore, more detailed analyses

* Corresponding author. Mailing address: Department of Plant and Microbial Biology, 111 Koshland Hall, University of California, Berkeley, CA 94720. Phone: (510) 642-3906. Fax: (510) 642-4995. E-mail: andyoj@berkeley.edu.

▽ Published ahead of print on 19 March 2008.

of the associations and biochemical functions of the TGB proteins are required to provide a refined understanding of the mechanisms whereby their movement processes are mediated.

Brakke et al. (7) have isolated a ribonucleoprotein (RNP) complex from BSMV-infected barley plants that contains a protein similar in size to the TGB1 protein. Although these experiments were conducted with wild-type (WT) virus, the ability of BSMV CP-deficient mutants to establish systemic infections provides strong evidence that virus movement occurs via an RNP complex (30). However, biochemical analyses of the RNP complex have not been conducted, so possible interactions of the TGB1 protein with viral RNAs or other TGB proteins are not understood. It is known however, that BSMV and the related hordeivirus PSLV TGB1 proteins are able to bind both single-stranded RNA and double-stranded RNA (dsRNA) with high affinity in vitro (10, 23). In addition, the BSMV TGB2 and TGB3 proteins are required for cell-to-cell movement (21, 30) but their presence in the RNP has not been investigated, nor are their interactions with TGB1 understood. Thus, several intriguing questions regarding the possible binding interactions of TGB proteins and the nature of the viral RNAs associated with RNP complexes need to be answered to understand the movement mechanisms of BSMV and other hordeiviruses. Therefore, we have characterized the BSMV TGB interactions in more detail and have analyzed the physical associations of the TGB proteins and the *cis* and *trans* expression requirements for cell-to-cell movement.

MATERIALS AND METHODS

In vitro transcription reactions and plant inoculations. Infectious BSMV ND18 RNA transcripts were generated from linearized cDNA templates by using T7 RNA polymerase as previously described by Petty et al. (33). The transcribed RNAs were diluted in GKP buffer (50 mM glycine, 30 mM $KHPO_4$, pH 9.2, 1% bentonite, 1% Celite) and used to inoculate barley (*Hordeum vulgare* cv. Black Hulless), *Nicotiana benthamiana*, and *Chenopodium amaranticolor* (33).

Isolation of an RNP complex from infected barley. The initial RNP complex isolation and sucrose density gradient procedures were modified from those described by Brakke et al. (7). For this purpose, ND18 RNAα and -γ were coinoculated to Black Hulless barley along with RNAβ(β8his6) containing mutations that eliminate CP expression and incorporate a six-residue histidine tag fused to the N terminus of TGB1 (10). Systemically infected leaf tissue (~400 mg) was harvested at 6 days postinoculation (dpi) and ground in 2 ml of isolation buffer (200 mM Tris, 60 mM KCl, 30 mM $MgCl_2$, 200 mM sucrose, 5 mM iodoacetamide, pH 8.5) at 4°C, followed by addition of 2 ml of isolation buffer containing 4% (vol/vol) Triton X-100. The crude extracts were centrifuged at 10,000 rpm for 10 min at 4°C. In experiments to examine the stability of the RNP complex, extracts were modified to achieve final concentrations of 100 mM NaCl, 300 mM NaCl, 500 mM NaCl, 25 mM EDTA, 50 mM EDTA, and 1% (wt/vol) sodium dodecyl sulfate (SDS). Upon addition of 100 to 500 mM NaCl, KCl was omitted from the buffer, and upon addition of 25 to 50 mM EDTA, $MgCl_2$ was omitted. The supernatants were recovered; loaded onto a sucrose gradient formed by layering 4, 8, 8, 8, and 5 ml of 15, 20, 30, 40, and 50% (wt/vol) sucrose in gradient buffer (50 mM glycine, 20 mM KCl, 5 mM $MgCl_2$, pH 8.5); and centrifuged at 26,000 rpm in a Beckman SW28 rotor for 5 h at 4°C. After centrifugation, the gradients were fractionated into 1.2-ml fractions with an ISCO (Instrumentation Specialties, Lincoln, NE) density gradient fractionator equipped with a UA5 UV monitor. A 100-μl aliquot was removed from each fraction for further analyses, and fractions 15 to 18, which contained high levels of the TGB1 protein, were pooled to give a total volume of approximately 4.5 ml. The pooled fractions were diluted with 20 ml of buffer A (200 mM Tris, 60 mM KCl, 30 mM $MgCl_2$, 0.1% [vol/vol] Triton X-100, pH 8.5) and applied to a 1-ml Ni-nitrilotriacetic acid agarose affinity column (Qiagen, Valencia, CA) equilibrated in buffer B (buffer A containing 200 mM sucrose). The column was washed with 20 ml of buffer B, followed by 10 ml of buffer B containing 40 mM imidazole. Proteins were eluted from the column with 10 ml of buffer B containing 150 mM imidazole. After ethanol precipitation, gradient and column fractions were analyzed for protein and RNA composition.

The precipitated samples were resuspended in AAE buffer [110 mM $(NH_4)_2CO_3$, 330 mM NH_4Cl, 11 mM EDTA, pH 9.3] containing 1% (wt/vol) SDS or protein extraction buffer (400 mM sucrose, 100 mM Tris, 10 mM KCl, 5 mM $MgCl_2$, 10% glycerol, 10 mM β-mercaptoethanol, 1 mM benzamidine, 1 mM phenylmethylsulfonyl fluoride, pH 7.5) (11) to analyze RNA or protein content, respectively. After gel electrophoresis RNAs were examined by Northern blot analysis as described previously (41) and protein composition was evaluated by silver staining or Western blot analysis (11).

BSMV cDNA constructs. The TGB1, TGB2, and TGB3 sequences were amplified from the BSMV β42SpI cDNA clone (32) with the primers shown in Table 1, and mutant derivatives of TGB2 and TGB3 were generated by a modified overlap extension PCR method (40). In order to introduce the TGB2 and TGB3 mutant sequences into a modified RNAβ cDNA clone, β42SpI was digested with NcoI after the *TGB1* promoter at position 802 (17) and PflMI at position 3041, and the mutant TGB sequences were ligated into these sites.

Chemical cross-linking. Cross-linking experiments with a tripeptide, GlyGlyHis (GGH), were modified from those of Fancy et al. (12) as described by Bragg and Jackson (5). BSMV-infected barley leaves (0.5 g) were extracted at 7 dpi by grinding in a mortar and pestle with cold nickel column buffer (100 mM Tris, pH 8.0, 200 mM NaCl, 30 mM $MgCl_2$, 0.1% Triton X-100) containing a cocktail of proteinase inhibitors (1 μg/ml each leupeptin, pepstatin, and aprotinin plus 50 μM phenylmethylsulfonyl fluoride) that had been added immediately before grinding. Tissue preparation, cross-linking reactions, and polyacrylamide gel electrophoresis (PAGE) were conducted after boiling in urea loading buffer (8 M urea, 20% glycerol, 6% β-mercaptoethanol, 100 mM Tris-HCl, pH 6.8) to dissociate nonspecific protein aggregates (5).

Affinity chromatography of TGB proteins. Glutathione *S*-transferase (GST) affinity assays were used to analyze physical interactions between the TGB proteins. For these assays, the TGB1 and TGB3 ORFs were amplified in PCRs and ligated in frame to the C terminus of the GST ORF at the BamHI and EcoRI restriction sites in plasmid pGEX-2T (Amersham, Piscataway, NJ) as described previously (13). GST-TGB1 and GST-TGB3 fusions were amplified and cloned into the SmaI and EcoRI sites of the pBEVY:GL vector (28) to yield the pBEVY:GL:GST-TGB1 and pBEVY:GL:GST-TGB3 plasmids. In other constructions, the TGB1 and TGB3 ORFs were amplified with primers designed to introduce 5′ BamHI and 3′ XbaI sites (Table 1). The *TGB2* gene was amplified with primers designed to introduce a 5′ BamHI site followed by a His tag as a fusion to the TGB2 protein and a 3′ XbaI site (Table 1). These products were then introduced into the corresponding sites of the pBEVYGT or pBEVYGU vector to yield plasmids pBEVYGT-TGB1, pBEVYGT:HisTGB2, and pBEVYGU:TGB3, respectively (Table 1). The TGB1 helicase mutants M2 (K259R), M3 (D339N, E340N), M5 (R368A), and M7 (E464A) were amplified by PCR with the primers listed in Table 1, and the products were cloned into the pCR BluntII TOPO vector. TGB1 mutant sequences were excised with BamHI (M2 and M3—one BamHI site was provided by the Topo vector) or with BamHI and XbaI (M5 and M7) and introduced into the corresponding sites of the pBEVYGT vector to yield pBEVYGT:M2, pBEVYGT:M3, pBEVYGT:M5, and pBEVYGT:M7.

For coexpression of the GST-TGB fusion proteins with unfused TGB proteins, yeast strain BJ2407 was transformed with pBEVY constructs (28). Yeast transformants were grown overnight in 2 ml of synthetic dropout (SD) glucose medium (0.67% Bacto-yeast nitrogen base minus amino acids plus 2% glucose), diluted in 20 ml of SD-galactose (0.67% Bacto-yeast nitrogen base minus amino acids, plus 2% galactose), and then grown for 36 h at 28°C. Cells were harvested by low speed centrifugation and disrupted by vortexing in yeast lysis buffer (0.3 M sorbitol, 0.1 M NaCl, 5 mM $MgCl_2$, 10 mM Tris-HCl, pH 7.4, 1 mM phenylmethylsulfonyl fluoride, 1 μg of antipain/ml, 1 μg of leupeptin/ml) in the presence of glass beads. The GST fusions and bound TGB proteins were purified by glutathione-Sepharose affinity chromatography (Pharmacia, Uppsala, Sweden) by elution with glutathione according to the manufacturer's instructions.

Yeast two-hybrid assays. Yeast two-hybrid vectors (16) were designed to produce a fusion of either the Gal4 activation domain (AD) or the Gal4 binding domain (BD) to the N terminus of the TGB protein to be tested for interactions. To construct fusions to the AD (pGADTGB2, pGADTGB3) or the BD (pGBDUTGB2, pGBDUTGB3), TGB sequences were amplified with the primers shown in Table 1. The TGB2 PCR products were introduced into the BamHI and PstI sites of pGBDU, and the TGB3 PCR products were inserted into the BamHI and PstI sites of plasmid pGAD (Table 1).

Deletion and site-specific mutant forms of TGB2 were generated by PCR with the primers in Table 1, and the resulting fragments were ligated into the BamHI and PstI sites of the pGBDU vector. The pGBDU:$TGB2_{1-122}$, pGBDU:$TGB2_{1-115}$, and pGBDU:$TGB2_{1-90}$ clones lack the C-terminal 9, 16, and 41 amino acids, and the

TABLE 1. Oligonucleotides used in this study

Clone	5′ Oligonucleotide	3′ Oligonucleotide	Change(s) and/or source
BSMV genomic RNA derivatives for *cis* and *trans* studies and overexpression studies			
$\beta_{T1ssmut}$	NA[a]	NA	TGB2 (K11Y, N12R) and TGB3 truncation at aa[b] 72, from βdCla1 and βcstop
$\beta_{T1\Delta 2,3}$	NA	NA	TGB2 and -3 ORFs are deleted; formerly β34.1
$\beta_{T2,3L}$	NA	NA	TGB1 is deleted and TGB2 and -3 are expressed from sgRNAβ2; formerly βΔ2.0
$\beta_{T2,3H}$	TGB2NcoIF, TGCCCATGGG GATGAAGACCACACAG TTGG	TGB3PflmIR, ACACTCCAT CATATGGTTGATGG	TGB1 is deleted and TGB2 and -3 are expressed from sgRNAβ1
β_{T2}	TGB2NcoIF, TGCCCATGGG GATGAAGACCACACAG TTGG	TGB2PflmIR, AGAGCCAA TGATATGGAGACTAGC CAAT	TGB1 and -3 are deleted and TGB2 is expressed from sgRNAβ1
β_{T3}	TGB3NcoIF, TGCCCATGGC AATGCCTCATCCCC TGGA	TGB3PflmIR, ACACTCCAT CATATGGTTGATGG	TGB1 and -2 are deleted and TGB3 is expressed from sgRNAβ1
β_{T3mut}	TGB3NcoIF, TGCCCATGGC AATGCCTCATCCCC TGGA	TGB3PflmIR, ACACTCCAT CATATGGTTGATGG	TGB1 and -2 are deleted and TGB3(P105R, I108R) is expressed from sgRNAβ1
β-$TGB2_{G40R,D41R}$	TGB2NcoIF, TGCCCATGGG GATGAAGACCACACAG TTGG	TGB2PflmIR, AGAGCCAA TGATATGGAGACTAGC CAAT	G40R and D41R
β-$TGB3_{P105R,I108R}$	TGB3NcoIF, TGCCCATGGC AATGCCTCATCCCC TGGA	TGB3PflmIR, ACACTCCAT CATATGGTTGATGG	P105R and I108R
Yeast two-hybrid studies			
pGAD:TGB1	NA		None (WT); from Bragg et al., 2003
GAD:TGB2/pGBDU:TGB2	TGB2BamHIF, GCGGATCC GGATGAGACCACAG TTGG	TGB2PstIR, TACTGCAGCT AGCCAATATCGCAT AGTG	None (WT)
pGBDU:$TGB2_{1-122}$	TGB2BamHIF, GCGGATCC GGATGAGACCACAG TTGG	$TGB2_{122R}$, TACTGCAGCT ATCGAGAATGTCCGT TAAG	C-terminal 9-aa deletion
pGBDU:$TGB2_{1-115}$	TGB2BamHIF, GCGGATCC GGATGAGACCACAG TTGG	$TGB2_{115R}$, TACTGCAGCT AGCCCTGACAGTCTT CTCC	C-terminal 16-aa deletion
pGBDU:$TGB2_{1-90}$	TGB2BamHIF, GCGGATCC GGATGAGACCACAG TTGG	$TGB2_{90R}$, TACTGCAGCTA TAAATAGGAAATGA TTCC	C-terminal 41-aa deletion
pGBDU:$TGB2_{11-90}$	$TGB2_{11F}$, GCGGATCCGGAT GAAGTATTGGCCAATT GTCGCCGGA	$TGB2_{90R}$, TACTGCAGCTA TAAATAGGAAATGA TTCC	N-terminal 10-aa and C-terminal 41-aa deletions
pGBDU:$TGB2_{G40R,D41R}$	TGB2BamHIF, GCGGATCC GGATGAGACCACAG TTGG	$TGB2_{40,41R}$, TTTGTGAATA TTACGGCGGGATT CCGT	G40R and D41R
	$TGB2_{40,41F}$, GAATCCCGCCG TAATATTCACAAATTC	TGB2PstIR, TACTGCAGCT AGCCAATATCGCAT AGTG	
pGBDU:$TGB2_{G40R}$	TGB2BamHIF, GCGGATCC GGATGAGACCACAG TTGG	$TGB2_{40R}$, TTTGTGAATAT TATCGCGGGATTCCGT	G40R
	$TGB2_{40F}$, GAATCCCGCGAT AATATTCACAAT	TGB2PstIR, TACTGCAGCT AGCCAATATCGCAT AGTG	
pGBDU:$TGB2_{D41R}$	TGB2BamHIF, GCGGATCC GGATGAGACCACAG TTGG	$TGB2_{41R}$, TTTGTGAATAT TACGGCCGGATTCCGT	D41R
	$TGB2_{41F}$, GAATCCGGCCGT AATATTCACAAATTC	TGB2PstIR, TACTGCAGCT AGCCAATATCGCAT AGTG	

Continued on following page

TABLE 1—*Continued*

Clone	5′ Oligonucleotide	3′ Oligonucleotide	Change(s) and/or source
pGBDU:TGB2$_{G49R,G50R}$	TGB2BamHIF, GCGGATCC GGATGAGACCACAG TTGG	TGB2$_{49,50R}$, TGACCCGTCC CTGTAACTACGTC GGTT	G49R and G50R
	TGB2$_{49,50F}$, CACAAATTCGC CAACCGACGTAGTTAC	TGB2PstIR, TACTGCAGCT AGCCAATATCGCAT AGTG	
pGAD:TGB3/pGBDU:TGB3	TGB3EcoRIF, CCGAATTCC TATGCCATCGGATCATT	TGB3PstIR, TTCTGCAGTT AGAGAAAAAAGCTTA ACGCAAAA	WT
pGAD:TGB3$_{1-89}$	pGAD:TGB3 digested with BglII and religated		C-terminal 66-aa deletion
pGAD:TGB3$_{16-155}$	TGB3$_{16F}$, CCGGATCCATGC CATCATCGGAATCATT	TGB3PstIR, TTCTGCAGTT AGAGAAAAAAGCTTA ACGCAAAA	N-terminal 15-aa deletion
pGAD:TGB3$_{1-149}$	TGB3EcoRIF, CCGAATTCC TATGCCATCGGATCATT	TGB3$_{149R}$, TACTGCAGTTA GAAAAAAGCTTAACG CAAAA	C-terminal 6-aa deletion
pGAD:TGB3$_{16-149}$	TGB3$_{16F}$, CCGGATCCATGC CATCATCGGAATCATT	TGB3$_{149R}$, TACTGCAGTTA GAAAAAAGCTTAACG CAAAA	N-terminal 15-aa and C-terminal 6-aa deletions
pGAD:TGB3$_{Q90Y,D91R,L92Y,D93R}$	TGB3$_{YRYRFor}$, TATCGTTAC CGGCGTGAAGATCTAT	TGB3PstIR, TTCTGCAGTT AGAGAAAAAAGCTTA ACGCAAAA	Q90Y, D91R, L92Y, D93R
	TGB3EcoRIF, CCGAATTCC TATGCCATCGGATCATT	TGB3$_{YRYRRev}$, CCGGTAAC GATAATAGAAGTAGG GACC	
pGAD:TGB3$_{P105R,I108R}$	TGB3BamHIF, CCGGATCC CTATGGCAATGCCTCA TCCC	TGB3$_{105,108R}$, ACGAACTTC TCGATTCGTAGCC	P105R, I108R
	TGB3$_{105,108F}$, AATCGAGAA GTTCGTGCGGCCATCCA	TGB3PstIR, TTCTGCAGTT ACCTTTTTGAAGAA AGTA	
pGAD:TGB3$_{P105R}$	TGB3BamHIF, CCGGATCC CTATGGCAATGCCTCA TCCC	TGB3$_{105R}$, AATAACTTCTC GATTCGTAGCC	P105R
	TGB3$_{105F}$, AATCGAGAAGT TATTGCGGCCATCCA	TGB3PstIR, TTCTGCAGTT ACCTTTTTGAAGAA AGTA	
pGAD:TGB3$_{I108R}$	TGB3BamHF, CCGGATCCC TATGGCAATGCCTCA TCCC	TGB3$_{108R}$, ACGAACTTCT GGATTCGTAGCC	I108R
	TGB3$_{108F}$, AATCCAGAAGT TCGTGCGGCCATCCA	TGB3PstIR, TTCTGCAGTT ACCTTTTTGAAGAA AGTA	
pGAD:TGB3$_{Q115Y,P118R,G120R}$	TGB3BamHIF, CCGGATCC CTATGGCAATGCCTCA TCCC	TGB3$_{115,118,120R}$, CCGAAAA CGGTACTTATACCAA TGGT	Q115Y, P118R, G120R
	TGB3$_{115,118,120F}$, TATAAGTA CCGTTTTCGGGAAT CTCC	TGB3PstIR, TTCTGCAGTT ACCTTTTTGAAGAA AGTA	
pGAD:TGB3$_{H5L,C11Y}$	TGB3$_{5,11F}$, CCGGATCCCTA TGGCAATGCCTCTTCCC CTGGAATGTTGT	TGB3PstIR, TTCTGCAGTT ACCTTTTTGAAGAA AGTA	H5L, C11Y
pGAD:TGB3$_{H5L,C9Y,C11Y}$	TGB3$_{5,9,11F}$, CCGGATCCCT ATGGCAATGCCTCTTCC CCTGGAATATTGT	TGB3PstIR, TTCTGCAGTT ACCTTTTTGAAGAA AGTA	H5L, C9Y, C11Y
GST pull-down experiments			
pBEVYGST	NA		From M. M. Goodin et al., 2001
pBEVYTGB1	TGB1BamHIF, CCGGATCC ATGGACATGACGAA AACT	TGBIXbaIR, GCTCTAGAT TATTTGGCCTTGAACC AACTG	None (WT)
pBEVYGST:TGB1	TGB1BamHIF, CCGGATCC ATGGACATGACGAA AACT	TGB1EcoRIR, TTGAATCC TTATTTGGCCTTGAAC CAACTGTG	GST fusion to N terminus of TGB1
	pGEXGST5′, GAGACCCGG GATGTCCCCTATACTAG GTTATTG	TGB1EcoRIR, TTGAATCC TTATTTGGCCTTGAAC CAACTGTG	

Continued on facing page

TABLE 1—*Continued*

Clone	5′ Oligonucleotide	3′ Oligonucleotide	Change(s) and/or source
pBEVYHis:TGB2	TGB2HisF, TTGGATCCCCA TGCATCACCATCACCAT CACAAGACCACAGTTG GTTCA	TGB2PstIR, TACTGCAGCT AGCCAATATCGCAT AGTG	N-terminal six-His tag
pBEVYGST:TGB3	TGB3BamHIF, CCGGATCC ATGGCAATGCCTCA TCCC	TGB3EcoRIR, TTGAATTC TTACCTTTTTGAAGAA AGTAAGAG	GST fusion to N terminus of TGB3
	pGEXGST5′, GAGACCCGG GATGTCCCCTATACTAG GTTATTG	TGB3EcoRIR, TTGAATTC TTACCTTTTTGAAGAA AGTAAGAG	
pBEVYGST:TGB1 (M2)	TGB1BamHIF, CCGGATCC ATGGACATGACGAA AACT	TGB1SpeIR, GCACTAGTT TATTTGGCCTTGAACC AACTGTG	TGB1 M2 mutant (K259A)
pBEVYGST:TGB1 (M3)	TGB1BamHIF, CCGGATCC ATGGACATGACGAA AACT	TGB1SpeIR, GCACTAGTT TATTTGGCCTTGAACC AACTGTG	TGB1 M3 mutant (D339N, E340N)
pBEVYGST:TGB1 (M5)	TGB1BamHIF, CCGGATCC ATGGACATGACGAA AACT	TGBIXbaIR, GCTCTAGAT TATTTGGCCTTGAACC AACTG	TGB1 M5 mutant (R368A)
pBEVYGST:TGB1 (M7)	TGB1BamHIF, CCGGATCC ATGGACATGACGAA AACT	TGBIXbaIR, GCTCTAGAT TATTTGGCCTTGAACC AACTG	TGB1 M7 mutant (R464A)

[a] NA, not applicable.
[b] aa, amino acid.

pGBDU:TGB2$_{11\text{-}90}$ derivative lacks the N-terminal 10 and C-terminal 41 amino acids of the protein. Overlap PCR was used to engineer the following site-specific mutations. The glycine 40 and aspartic acid 41 residues were changed to arginine to construct the pGBDU:TGB2$_{G40R,D41R}$ derivative. In the pGBDU:TGB2$_{G40R}$ mutant, glycine 40 was changed to arginine, and in pGBDU:TGB2$_{D41R}$, aspartic acid 41 was changed to arginine. The pGBDU:TGB2$_{G49R,D50R}$ derivative contains arginine substitutions for the glycine 49 and aspartic acid 50 residues.

Additional mutations were incorporated into TGB3 by PCR with the primers listed in Table 1, and the resulting fragments were ligated into the BamHI and PstI sites of the pGAD vector. The pGAD:TGB3$_{1\text{-}150}$ and pGAD:TGB3$_{1\text{-}89}$ clones lack the C-terminal 5 and 66 amino acids. The pGAD:TGB3$_{16\text{-}155}$ clone has a deletion of the N-terminal 15 amino acids, and the pGAD:TGB3$_{16\text{-}150}$ derivative lacks the N-terminal 15 and C-terminal 5 residues. Overlap PCR was used to introduce the following site-specific mutations. The pGAD:TGB3$_{Q90Y,D91R,L92Y,N93R}$ mutant has tyrosine substitutions for the glutamine 90 and leucine 92 residues and arginine substitutions for the aspartic acid 91 and asparagine 93 residues. Proline 105 and isoleucine 108 were changed to arginine in the pGAD:TGB3$_{P105R,I108R}$ derivative. These mutations were also individually introduced into the pGAD:TGB3$_{P105R}$ and pGAD:TGB3$_{I108R}$ clones. The pGAD:TGB3$_{Q115Y,P118R,G120R}$ mutant has a tyrosine substitution for glutamine 115 and arginines for proline 118 and glycine 120. The pGAD:TGB3$_{H5L,C11Y}$ clone contains a leucine substitution for histidine 5 and a tyrosine for cysteine 11, and the pGAD:TGB3$_{H5L,C9Y,C11Y}$ mutant contains an additional tyrosine substitution for cysteine 9.

Yeast strain PJ69-4A was transformed with *LEU2*-selected AD and *URA3*-selected BD constructs as previously described (2). To select for transformants containing the AD and BD plasmids, yeast cells were plated on SD-glucose medium containing 20 mg/liter Ade, His, Met, and Trp and 30 mg/liter Lys and grown for 3 days at 28°C. Yeast colonies were tested for interactions by expression of the reporter genes *ADE2* and *HIS3* after being streaked onto SD-glucose medium containing 20 mg/liter Met and Trp and 30 mg/liter Lys and growing for 3 to 5 days at 28°C or at room temperature.

Western blot detection of GST fusion and six-His-tagged proteins. Green fluorescent protein (GFP) fusion proteins and His-tagged proteins were extracted from leaf samples and detected via Western blotting. GST fusion proteins (GST-TGB1, GST-TGB3, and GST), TGB1, and His-TGB2 were extracted from yeast as described by Goodin et al. (13). Leaves from *C. amaranticolor* and barley plants inoculated with infectious BSMV transcripts were analyzed at 10 dpi. Protein samples were mixed in equal volumes of Laemmli loading buffer (100 mM Tris-Cl, pH 6.8, 4% SDS, 0.2% bromophenol blue, 20% glycerol, 200 mM β-mercaptoethanol), heated to 95°C for 10 min, and separated by 8 or 10% SDS-PAGE. After transfer to nitrocellulose membranes, proteins were detected as appropriate, with a polyclonal mouse TGB1 antibody used in our previous studies (10), an anti-GST polyclonal antibody (Sigma, St. Louis, MO), an H15 His-probe polyclonal antibody (Santa Cruz Biotechnology, Santa Cruz, CA), and goat anti-rabbit or anti-mouse horseradish peroxidase conjugate, as appropriate.

Reverse transcription (RT)-PCR analyses. To detect BSMV RNA derivatives, total RNA was extracted from 100 mg of finely powdered tissue with the Qiagen RNeasy Plant Mini Kit, and DNA was removed by on-column DNase digestion according to the manufacturer's specifications (Qiagen, Carlsbad, CA). Total RNA (2 μg) was used for reverse transcription with the BSMV3′ primer (5′TG CAAACACTCCCATCATATG 3′), and PCR amplifications (50-s extension, 35 cycles) were performed with the CP5′ (5′ TTGGATCCATGCCGAACGTTTC TTTGAC 3′) and TGB3′ (5′ CCTTTTTGAAGAAAGTAAGAG 3′) or CP5′ and CP3′ (5′ ACCTGCAGTCACGCTTCCTCGGCATC 3′) oligomers.

***RNAβ cis* and *trans* expression constructs.** The β$_{T1ssmut}$ derivative is a combination of the βCla and βΔ3.1 clones previously described by Petty et al. (31). The βCla mutant contains site-specific mutations in the TGB2 ORF (residues 11 and 12 were changed from KY to NR), and the βΔ3.1 clone introduces a premature stop codon in the TGB3 ORF that truncates the protein at amino acid 72. The β$_{T1\Delta2,3}$ derivative was previously described as βΔ34.1 (31). In this construct, the overlapping TGB2/3 ORFs were deleted completely. Two constructs were also designed to permit *cis* expression of the TGB2 and TGB3 proteins. The β$_{T2,3L}$ construct was previously described as βΔ2.0 (31) and contains a 572-nucleotide (nt) deletion (from the NcoI site, which overlaps the TGB1 start site, to the SalI site) to eliminate expression of the TGB1 ORF. In this derivative, the normally low-abundance *TGB2* and *-3* genes remain under the control of the *sgRNAβ2* promoter (17). The β$_{T2,3H}$ derivative mediates the expression of TGB2 and TGB3 in *cis* under the control of the *sgRNAβ1* promoter. To generate β$_{T2,3H}$, the three TGB ORFs were removed by a deletion from the NcoI site to the PflMI site that encompasses positions 802 to 3041. The overlapping TGB2 and -3 ORFs were then amplified by PCR (Table 1) and inserted at the NcoI and PflMI sites. For derivatives modified for expression of the TGB2 and -3 proteins in *trans*, mutants β$_{T2}$, β$_{T3}$, and β$_{T3mut}$ (which contains site-specific P105R and I108R mutations in TGB3) were constructed similarly to the β$_{T2,3H}$ clone by placing the PCR-amplified TGB2 or TGB3 ORF (Table 1) under the control of the *sgRNAβ1* promoter at the NcoI site.

RESULTS

TGB1 and BSMV plus-sense RNAs are the major components of an RNP complex present in BSMV-infected barley. BSMV and other viruses expressing hordeivirus-like (class I)

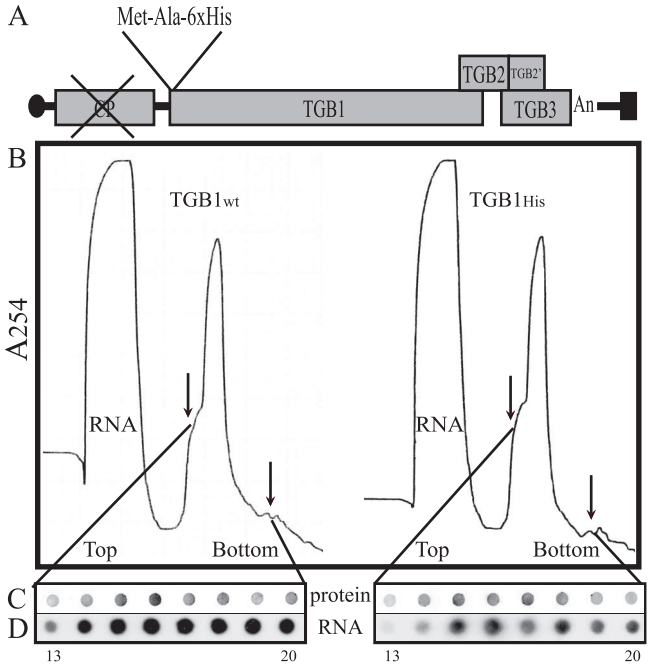

FIG. 1. Analysis of a nucleoprotein complex present in BSMV-infected plants. (A) BSMV RNAβ containing a deletion in the CP ORF and a His-tagged TGB1 protein. (B) Sedimentation of nucleoprotein complexes isolated from BSMV-infected plants expressing a $TGB1_{wt}$ or TGB_{His} derivative. (C) Immunoblot assays with TGB1 antiserum to proteins present in fractions 13 to 20 collected from the major peaks of A_{254}. (D) Dot blot assay of BSMV RNAs in fractions 13 to 20 visualized with a ^{32}P-labeled riboprobe complementary to the conserved 238-nt 3′ termini of the BSMV gRNA and sgRNA.

TGB MPs have been postulated to move from cell to cell as RNP complexes consisting of viral RNA and one or more of the TGB proteins (29, 30). This hypothesis was supported by the experiments of Brakke et al. (7), who previously detected an RNP in infected plants that contained BSMV RNA and a virus-specific 60-kDA protein, which we presume to be the TGB1 protein. However, the purity of the complex was compromised by the presence of virions and by host components. Thus, a number of questions exist about the viral and host proteins associated with the complex and the nature of the encapsidated RNAs. Therefore, we constructed a BSMV mutant derivative that is unable to express the CP and encodes an N-terminally His-tagged TGB1 protein (Fig. 1A). This provides a system that permits extensive purification of a CP-deficient RNP by a two-step procedure involving sucrose density gradient fractionation and affinity chromatography.

To isolate the RNP, barley was coinoculated with the α and γ RNAs along with the RNAβ B7.β8 derivative ($TGB1_{wt}$), which encodes the WTTGB1 protein, or the B7.β8His6 derivative ($TGB1_{His}$), which expresses a TGB1 protein containing an N-terminal six-His tag (Fig. 1A) to permit Ni^{2+} affinity chromatography (10). Both mutant viruses are deficient in CP production, and hence, neither derivative can form virions (31). The mutants were able to establish systemic infections, and inoculated plants exhibited acute mosaic symptoms by 4 to 5 dpi. By 7 dpi, the systemically infected leaves developed severe striping and mild necrosis (data not shown). For RNP purification, systemically infected leaves were extracted at 6 dpi, when high levels of TGB1 were present in the tissue (11). Sucrose density gradient fractionation revealed a heterodisperse sedimenting component consisting of a major peak with a pronounced slowly sedimenting shoulder in plants infected with both the $TGB1_{wt}$ and $TGB1_{His}$ mutant viruses (Fig. 1B), but this component was not present in uninfected plants (data not shown). Western blot analyses of sucrose gradient fractions loaded with extracts from infected plants revealed that the TGB1 proteins were present at the highest levels in fractions 15 to 18 (Fig. 1C). When antiserum raised against a penta-His peptide was used to analyze extracts of $TGB1_{His}$ virus-infected plants, the same pattern was observed but the signal was not present in extracts from plants containing the $TGB1_{wt}$ protein (data not shown).

Sedimentation of viral RNAs across the gradients was evaluated by hybridization to a ^{32}P-labeled riboprobe complementary to the conserved 238-nt 3′-terminal region of each of the BSMV genomic RNAs (gRNAs) and sgRNAs. These dot blot analyses revealed that the greatest amounts of viral RNAs cosedimented with the TGB1 proteins (Fig. 1D). Therefore, pooled fractions 15 to 18, containing the maximal amounts of $TGB1_{wt}$ or $TGB1_{His}$, were subjected to Ni^{2+} affinity chromatography and the proteins eluting from the column were assessed by cross-reactivity with antiserum raised to TGB1 (Fig. 2A) or the penta-His peptide (data not shown). As expected, the $TGB1_{His}$ protein was retained on the column, whereas the $TGB1_{wt}$ protein failed to bind to the Ni affinity matrix (Fig. 2A). Dot blot hybridization of the column eluates with the BSMV 3′-specific probes revealed that BSMV RNAs were present only in $TGB1_{His}$ fractions (Fig. 2B). These results indicate that the affinity fractionation was specific for the $TGB1_{His}$ protein and suggest that BSMV RNAs are associated with TGB1.

We have previously shown that the TGB1 protein has a strong binding affinity for dsRNAs (10), raising the possibility that the RNP might contain replicative intermediates. To test this hypothesis, RNA associated with the RNP was subjected to Northern blot analyses with probes designed to detect the 238-nt conserved region of the BSMV RNAs in either the positive-sense or the negative-sense orientation. The results shown in Fig. 2C clearly demonstrate that the RNP contains only positive-sense RNAs with sizes corresponding to the BSMV gRNAs and sgRNAs. The presence of both gRNAs and sgRNAs suggests that a common RNA sequence, possibly the 3′ tRNA-like structure, may be involved in TGB1 interactions needed for the formation of the RNP in vivo. Moreover, the distinct shoulder consistently appearing in the RNP complex sedimentation profiles (Fig. 1B) suggests that the complexes are heterogeneous, so we presume that the gRNAs and sgRNAs are individually encapsidated by TGB1 to form separate nucleocapsids.

To further investigate the composition of the isolated RNP, proteins were resolved by SDS-PAGE and analyzed for additional host- and virus-encoded proteins by silver staining or Western blot analyses. Silver staining revealed a major protein corresponding in size to the TGB1 protein, and Western blot analyses verified that this band contained TGB1 (Fig. 2D). A few minor high-molecular-weight bands (>200 kDa) were also present near the top of the silver-stained gel, but these com-

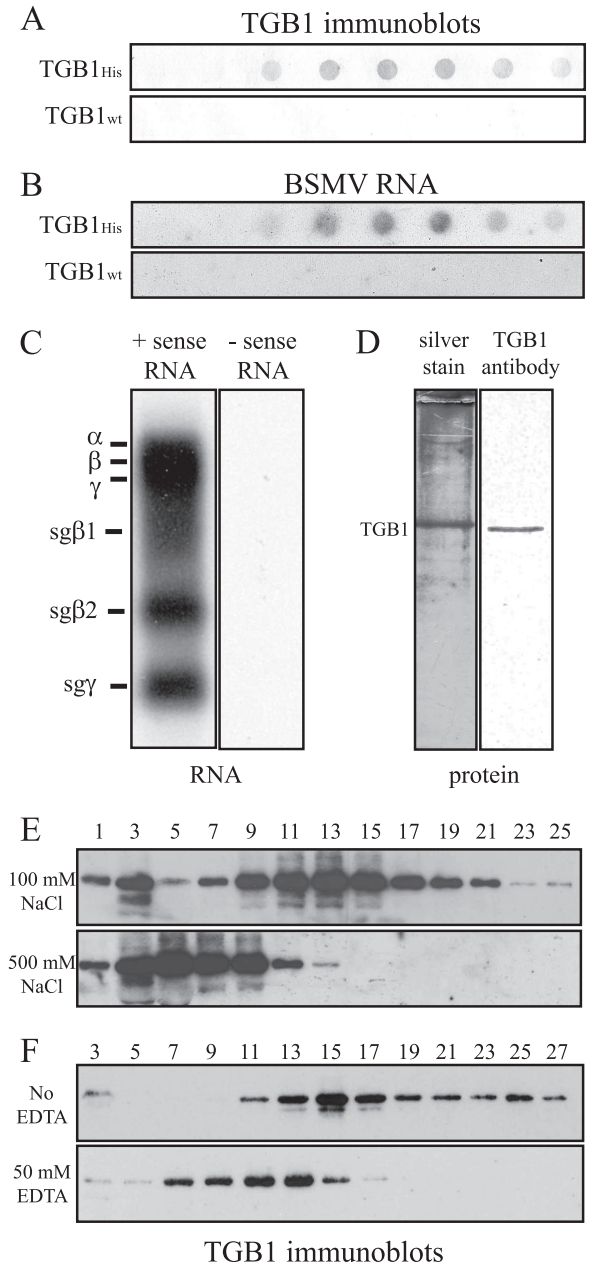

FIG. 2. Composition and stability of $TGB1_{wt}$ and $TGB1_{His}$ complexes recovered after metal affinity chromatography of pooled sucrose density gradient fractions 15 to 18. (A) Immunoblot analyses of metal affinity chromatography fractions with TGB1 antiserum. (B) Dot blot analyses of BSMV RNAs present in metal affinity chromatography fractions with a ^{32}P-labeled riboprobe complementary to the conserved 238-nt 3′ termini of the BSMV gRNA and sgRNA. (C) Northern blot analyses of RNAs recovered after metal affinity chromatography with ^{32}P riboprobes complementary to plus- or minus-sense BSMV RNA 3′ termini. (D) Polyacrylamide gel analyses of proteins recovered after metal affinity chromatography by silver staining and Western blotting with TGB1 antibody. (E and F) Western blot assays with TGB1 antisera of BSMV nucleoprotein complexes after sucrose density gradient fractionation in the presence of 100 or 500 mM NaCl (E) or in the presence or absence of 50 mM EGTA (F). Note that in panel C, the designations α, β, and γ to the left of the panel refer to the electrophoresis of BSMV RNA.

ponents are several times larger than TGB1. In addition, examination of more rapidly migrating components indicated that the TGB2 and TGB3 proteins were not present in detectable amounts. Western blot analyses with antisera raised to TGB2 and other virus-encoded proteins, αa, TGB2, γa, or γb, failed to reveal additional BSMV-encoded proteins (data not shown). Thus, our results, in toto, indicate that the RNP consists primarily of TGB1 protein bound to positive-sense BSMV gRNA and sgRNA and does not contain minus-sense BSMV RNAs, dsRNAs, or substantial amounts of host-encoded proteins.

With in vitro RNA binding assays, we previously found that TGB1 bound to RNA at NaCl concentrations below 300 mM, but binding was not observed in 400 and 500 mM NaCl (10). To determine whether the nucleoprotein complexes were salt stable and hence similar to our previous in vitro binding results, we investigated the stability of the in vivo-formed TGB1/RNA complex by extraction in buffers that contained either 100 or 500 mM NaCl. The extracts were then subjected to sucrose density gradient centrifugation, and the sedimentation of the TGB1 protein into the gradients was evaluated by Western blot analyses. At 100 mM NaCl, the maximal concentrations of TGB1 were found in fractions 9 to 17, while at 500 mM NaCl, TGB1 was found at maximal levels in fractions 3 to 9 (Fig. 2E). The shift of the TGB1 protein to a higher position in the gradient after high-salt treatment indicates that the nucleoprotein from infected tissue is stable within the range of physiological NaCl levels but is disrupted at higher salt concentrations. A smaller shift in sedimentation was observed when EDTA was added to the protein extraction buffer, suggesting that divalent metal interactions may be important for the stability of the complexes. In these samples, the peak shifted from fractions 13 to 17 in the absence of EDTA to fractions 7 to 15 in the presence of 50 mM EDTA (Fig. 2F). In contrast, TGB1 remained at the top of the gradient when 1% SDS was added to the extraction buffers, indicating that detergent treatment completely disrupts the RNP (data not shown).

TGB1 participates in homologous binding interactions. The presence of a TGB1 RNP in infected plants suggests strongly that TGB1 engages in homologous interactions and that such interactions are required for cell-to-cell movement. To identify TGB1 interactions that might be present in infected plants, chemical cross-linking experiments were conducted. For these experiments, a diffusible GGH tripeptide cross-linking agent was used that results in covalent coupling of closely associated proteins after addition of nickel and a peracid catalyst (12). In the results shown in Fig. 3, BSMV-infected barley extracts were recovered and not treated; treated with Ni^{2+}, the peracid, and the cross-linking agent; or exposed to Ni^{2+} and the catalyst alone. In the untreated extracts (left lane) and in extracts containing Ni^{2+} and the catalyst alone (right lane), the TGB1 protein was present only as the monomer form in the SDS gels (Fig. 3). However, the TGB1 protein was converted to a high-molecular-weight complex that moved near the top of the gels after the addition of Ni^{2+} and the GGH cross-linker (Fig. 3, center lane). Although our cross-linking results indicate that TGB1 forms complexes in infected cells, the nature of these complexes is not clear and it is possible that several different types of virus- and/or host-specific interactions exist.

A series of gel electrophoresis experiments by Leshchiner et

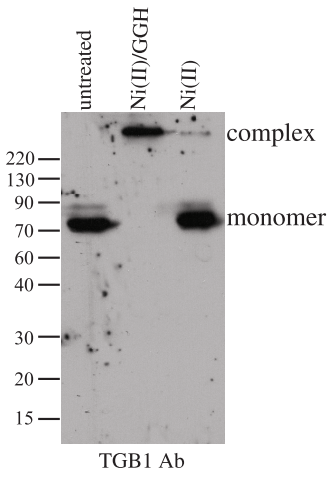

FIG. 3. TGB1 interactions present in Ni(II)/GGH-cross-linked extracts from BSMV-infected plants. Extracts recovered at 7 dpi were treated as follows: lane 1, no cross-linking; lane 2, cross-linking with Ni(II)/GGH; lane 3, treatment with Ni(II) in the absence of GGH. Treated samples were heated in the presence of SDS and 8 M urea, separated on polyacrylamide gels, blotted to nitrocellulose, and visualized with TGB1 antisera. Ab, antibody. The values on the left are molecular sizes in kilodaltons.

al. (23) have previously suggested that the PSLV TGB1 helicase region might be important for homologous TGB1 interactions. Although the full-length 63-kDA PSLV TGB1 protein appeared to have relatively weak homologous interactions, strong interactions were observed for a 113-amino-acid TGB1 fragment that contained only helicase motifs 1, 1a, and 2 (23). Of particular interest was the unusual resistance of the truncation mutants to SDS, which we have previously shown to be a nonspecific aggregation hallmark of other BSMV proteins (5). Therefore, because site-specific mutations within the helicase motifs were not tested in the experiments of Leshchiner et al., a bona fide contribution of the helicase sequence to the formation of putative TGB1 dimers cannot be distinguished from nonspecific interactions that may be a result of aberrant protein folding or other nonspecific interactions.

To provide a more definitive analysis of TGB1 interactions, we used GST affinity chromatography to assess physical associations of the WT TGB1 protein and several site-specific helicase mutants that are known to inactivate cell-to-cell movement (21). Proteins were expressed in yeast cells transformed with pBEVY plasmids that can be maintained under leucine selection for simultaneous and constitutive expression of approximately equimolar amounts of protein (28). For these experiments, a GST-TGB1 fusion protein and a native or mutant TGB1 protein were coexpressed, and GST affinity chromatography was used to purify the proteins extracted from transformed yeast cells. In TGB1-TGB1 homologous-interaction tests, the native TGB1 protein was retained on and eluted from the affinity column when it was coexpressed with GST-TGB1, but as expected, the protein passed through the column when expressed with unfused GST (Fig. 4, lanes 1 and 2) or when it was expressed alone (data not shown). Similar binding results were obtained with the TGB1 substitution mutants that targeted the helicase R368 (M5 mutant, motif IV) and R464 (M7 mutant, motif VI) residues within the respective conserved motifs. However, the N-terminal M2 (K259A) or M3 (D339N, E340N) mutant helicase that contained residue substitutions within helicase motif I or II failed to participate in homologous binding (Fig. 4C and D). These results thus agree with those of Leshchiner et al. (23) and provide additional information demonstrating that conserved helicase motifs I and II are each required for homologous TGB1 interactions.

TGB1 interacts with TGB3 but not TGB2. To evaluate heterologous interactions of TGB1 with TGB2 or TGB3, the His-TGB2 and GST-TGB3 fusion proteins were constructed. In these experiments, TGB1 was retained on the glutathione affinity column by GST-TGB3 but failed to bind when coexpressed with GST (Fig. 4B, lanes 3 and 4). In contrast, His-TGB2 was not recovered after affinity chromatography in the presence of GST-TGB1 (Fig. 4B, lane 6). These results demonstrate heterologous TGB1-TGB3 binding and suggest that TGB1 and TGB2 do not engage in heterologous interactions.

TGB2 and TGB3 participate in heterologous binding. Affinity chromatography experiments were also carried out to investigate TGB2 and TGB3 binding. In these experiments, a TGB2 derivative containing an N-terminal His tag (His-TGB2) was recovered after coexpression with GST-TGB3 but not during expression with GST (Fig. 4, lanes 5 and 7) or when expressed alone (data not shown). However, yeast transformed with pBEVY vectors designed to express GST-TGB2, His-TGB3, and TGB3-His fusions failed to grow in tests to evaluate potential self-interactions of TGB2 and TGB3. Therefore, we were unable to test homologous pairings of TGB2 and TGB3 by affinity chromatography in the yeast expression system. In addition, pairing of AD-TGB2 and BD-TGB2 in the yeast two-hybrid system indicated that TGB2 does not participate in detectable homologous interactions in this system. Our affinity chromatography results thus provide evidence for specific heterologous TGB2-TGB3 interactions, but we were unable to identify homologous TGB2 or TGB3 interactions.

Additional yeast two-hybrid experiments verified the TGB2-TGB3 interactions identified by affinity chromatography of the GST fusion proteins. Yeast cotransformed with the AD-TGB3 and BD-TGB2 plasmids exhibited strong growth that was not observed in negative control experiments for these two plasmids (Table 2). To define the amino acids contributing to the TGB2-TGB3 interactions, several mutants were constructed and evaluated more extensively (Fig. 5). For this purpose, we engineered four BD-TGB2 fusions consisting of two TGB2 deletion mutants ($TGB2_{1\text{-}122}$ and $TGB2_{1\text{-}115}$) lacking the 9 or 41 C-terminal amino acids, respectively, and two derivatives ($TGB2_{1\text{-}90}$ and $TGB2_{11\text{-}90}$) with deletions in the 10 N-terminal residues or both the 10 and 41 C-terminal residues (Fig. 5). Each of these derivatives supported yeast growth when paired with the AD-TGB3 fusion and hence was competent to interact with TGB3. These results indicated that the TGB2 region functioning in heterologous binding to TGB3 resides between amino acids 11 and 90 and that the predicted C-terminal cytosolic sequences downstream of the second membrane-spanning domain are dispensable for heterologous binding.

We also generated additional site-specific mutations that targeted residues 11 to 90 of the full-length TGB2 protein that are conserved among the BSMV, LRSV, and PSLV proteins (Fig. 5). Among these substitutions, the $TGB2_{G40R,D41R}$ mutant that introduces two basic substitutions into the central

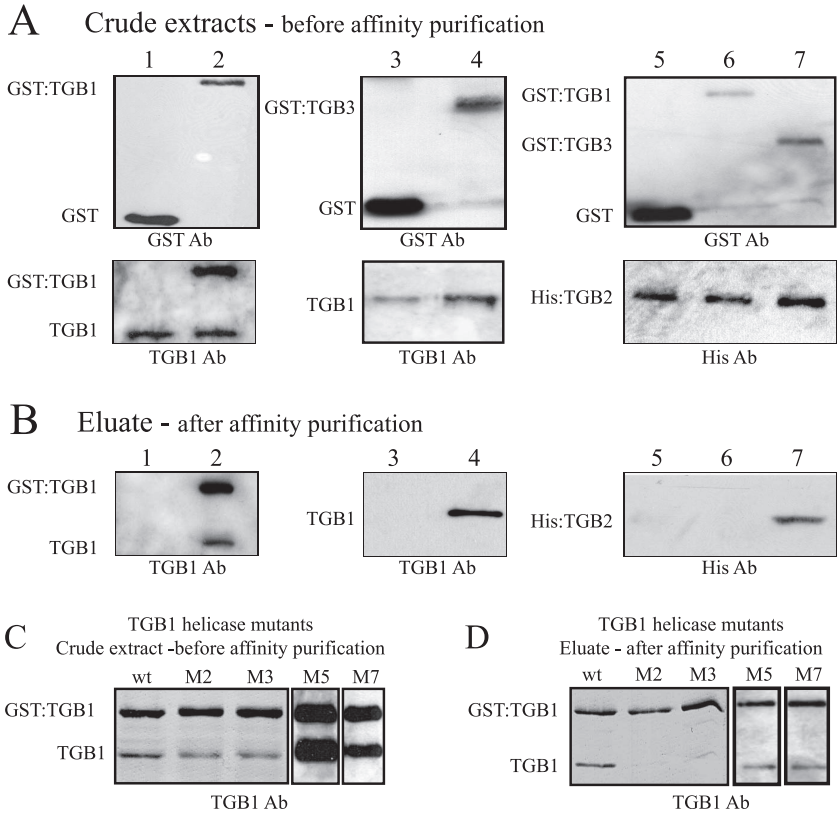

FIG. 4. Glutathione affinity chromatography detection of TGB protein interactions. TGB proteins were expressed in yeast cells, and protein extracts were separated by SDS-PAGE before (panels A and C, crude extracts) and after (panels B and D, column eluates) glutathione affinity chromatography. Proteins were reacted with anti-TGB1 and visualized with a goat anti-mouse secondary antibody (Ab) linked to horseradish peroxidase or with an anti-GST or anti-poly-His primary antibody reacted with a rabbit secondary antibody. (A and B) Proteins were coexpressed in the following combinations: lane 1, GST and TGB1; lane 2, GST-TGB1 and TGB1; lane 3, GST and TGB1; lane 4, GST-TGB3 and TGB1; lane 5, GST and His-TGB2; lane 6, GST-TGB1 and HisTGB2; lane 7, GST-TGB3 and His-TGB2. (C and D) GST-TGB1 was coexpressed in yeast with WT TGB1 or one of the mutant TGB1 proteins containing substitutions within conserved motif 1, 2, 4, or 6 of the helicase domain. Crude extracts (C) were subjected to glutathione affinity chromatography (D) to determine whether the mutant helicases were competent to interact with GST-TGB1. Note that the crude extract panels represent ~12% of the total protein extracted from yeast and ~80% of the total protein extracted was applied to the GSH matrix. The eluate panels were loaded with ~30% of the protein eluting from the GSH matrix. Therefore, we estimate that ~50% of the protein applied to the GSH was bound to the column and recovered during elution. The boxed regions show extracts that were fractionated on different gels.

hydrophilic region of the protein failed to elicit yeast growth when paired with TGB3, but the $TGB2_{G49R,G50R}$ mutant maintained its binding capability (Table 2). The G40R and D41R mutations were then introduced separately into BD-TGB2. The aspartic acid mutant $TGB2_{D41R}$ elicited yeast growth when paired with TGB3, but an arginine-for-glycine substitution ($TGB2_{G40R}$) to increase the polarity and charge at residue 40 was unable to support yeast growth. These data suggest that the G40 residue that is predicted to reside within the ER lumen is essential for interactions with TGB3 (Fig. 5).

A mutagenesis strategy similar to that undertaken with TGB2 was used to identify regions of the AD-TGB3 protein required for interactions with TGB2. Among these derivatives, the $TGB3_{1-89}$ deletion mutant, in which the C-terminal 66 amino acids had been truncated, failed to interact with WT TGB2 (Table 2). However, $TGB3_{16-155}$, $TGB3_{1-150}$, and $TGB3_{16-150}$ elicited yeast growth during interactions with WT TGB2. These results suggest that the region mediating TGB2 interactions resides between residues 89 and 150 of TGB3.

Five site-specific mutants containing altered amino acids that reside within the central cytoplasmic domain between the two hydrophobic membrane-spanning domains and that are conserved among the BSMV, LRSV, and PSLV TGB3 sequences were also tested in yeast two-hybrid interactions with TGB2 (Fig. 5). These mutants were designated $TGB3_{Q90Y,D91R,L92Y,N93R}$,

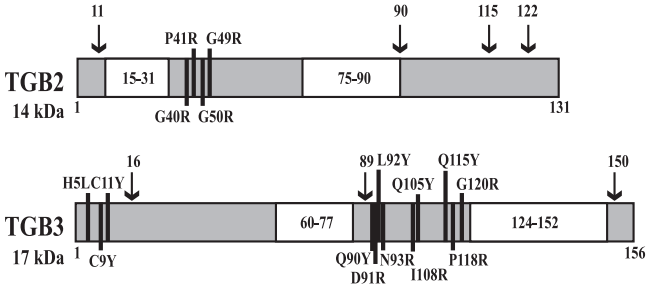

FIG. 5. Deletions and site-specific mutations introduced into the TGB2 and TGB3 proteins to assess yeast two-hybrid interactions and infectivity of the mutant proteins. Arrows above the drawings denote deletion sites. Solid lines extending above or below the rectangles illustrate the locations of site-specific amino acid substitutions, and white boxes represent the membrane-spanning domains within the proteins.

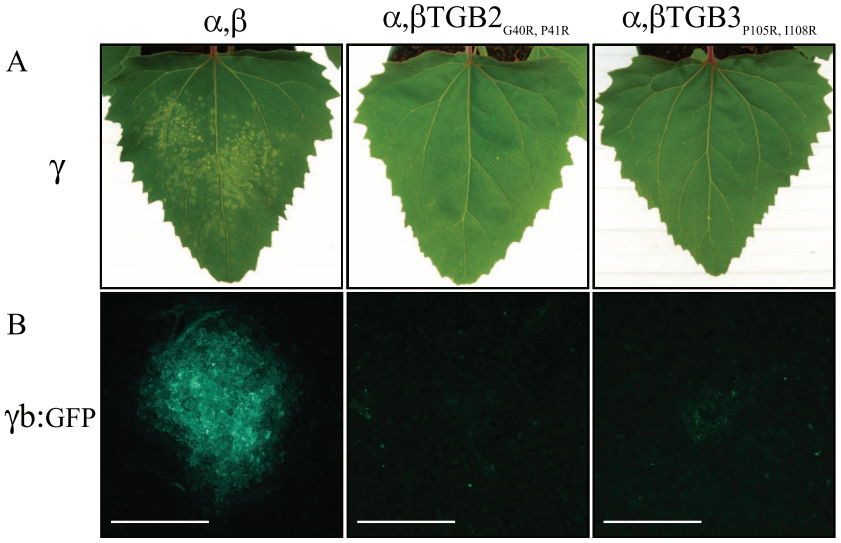

FIG. 6. Cell-to-cell movement of BSMV derivatives containing the $TGB2_{G40R,P41R}$ and $TGB3_{P105R,I108R}$ mutations. (A) *C. amaranticolor* leaves inoculated with infectious transcripts of WT RNAα and WT RNAγ or (B) *N. benthamiana* leaves inoculated with WT RNAα and RNAγ-γb-GFP plus either $RNAβ_{WT}$ or RNAβ transcripts containing the $TGB2_{G40R,P41R}$ and $TGB3_{P105R,I108R}$ mutations that disrupt TGB2 and TGB3 heterologous interactions. Photographs were taken at 12 dpi. Note that the small fluorescing spots in the γb-GFP panels represent fluorescence from single cells infected with inocula containing the TGB2 and TGB3 mutant proteins.

$TGB3_{P105R,I108R}$, $TGB3_{Q115Y,P118R,G120R}$, $TGB3_{H5L,C11Y}$, and $TGB3_{H5L,C9Y,C11Y}$. Of the five mutants, only $TGB3_{P105R,I108R}$ failed to support yeast growth (Table 2). The P105R and I108R substitutions were then introduced separately into the TGB3 sequence and tested for interactions with TGB2. The $TGB3_{P105R}$ derivative was competent to interact with TGB2, but the $TGB3_{I108R}$ mutant failed to elicit yeast growth, indicating that residue 108 within the cytoplasmic TGB3 domain is important for TGB2 interactions.

TABLE 2. Yeast two-hybrid interactions of BSMV TGB proteins

BD fusion	AD fusion	Interaction
TGB3		False positive
TGB1	TGB1	No colonies
TGB1	TGB2	No colonies
TGB1	TGB3	No colonies
TGB2	TGB2	−
TGB2	TGB1	−
TGB2	TGB3	+
$TGB2_{11-90}$	TGB3	+
$TGB2_{G40R,D41R}$	TGB3	−
$TGB2_{G40R}$	TGB3	−
$TGB2_{D41R}$	TGB3	+
$TGB2_{G49R,G50R}$	TGB3	+
TGB2	$TGB3_{1-89}$	−
TGB2	$TGB3P_{105R,I108R}$	−
TGB2	$TGB3_{P105R}$	+
TGB2	$TGB3_{I108R}$	−
TGB2	$TGB3_{H5L,C11Y}$	+
TGB2	$TGB3_{H5L,C9Y,C11Y}$	+
TGB2	$TGB3_{Q90Y,D91R,L92Y,D93R}$	+
TGB2	$TGB3_{Q115Y,P118R,G120R}$	+
TGB2	$TGB3_{16-150}$	+
TGB2	$TGB3_{1-150}$	+
TGB2	$TGB3_{16-155}$	+

Mutations affecting interactions of TGB2 and TGB3 abrogate cell-to-cell movement. To assess the effects of the $TGB2_{G40R,D41R}$ and $TGB3_{P105R,I108R}$ mutations on BSMV movement, we introduced these mutations into the RNAβ cDNA clone and inoculated barley and *C. amaranticolor* with WT RNAα and -γ and the RNAβ transcripts containing the TGB2 or TGB3 mutant derivative. The WT transcripts elicited the characteristic mosaic and striping symptoms in barley (data not shown) and necrotic lesions in *C. amaranticolor* that are typically associated with BSMV infection (Fig. 6A). In contrast, transcripts containing the derivative $TGB2_{G40R,D41R}$ or $TGB3_{P105R,I108R}$ failed to elicit discernible symptoms in either *C. amaranticolor* (Fig. 6A) or barley (data not shown).

Transcripts of WT RNAβ ($RNAβ_{wt}$) or RNAβ derivatives containing the site-specific $TGB2_{G40R,D41R}$ and $TGB3_{P105R,I108R}$ mutations were also inoculated into *N. benthamiana* leaves along with WT RNAα and RNAγb-GFP to provide a visual marker to assess virus spread. When $RNAβ_{wt}$ was used in inoculations, GFP fluorescence was observed at 12 dpi in foci measuring approximately 100 μm in diameter, indicating that the virus was able to move from the initially infected cells (Fig. 6B). In contrast, spreading fluorescent foci were not observed when either the $TGB2_{G40R,D41R}$ or the $TGB3_{P105R,I108R}$ mutant RNAβ derivative was tested. These results verify the *C. amaranticolor* and barley infectivity experiments and demonstrate that the residues required for TGB2-TGB3 interactions are also critical for cell-to-cell movement of BSMV (Fig. 6B).

Elevated expression of TGB3 is detrimental to BSMV cell-to-cell movement. TGB3 is expressed at levels approximately 10-fold lower than TGB2 during in vitro translation experiments and in protoplast reporter gene assays (41). Our results showing that interactions of TGB2 and TGB3 affect virus movement raised questions about the extent to which the relative levels of expression of TGB2 and TGB3 affect cell-to-cell

movement. These questions were also reinforced by beet necrotic yellow vein virus (BNYVV) experiments, suggesting that TGB3 complements the cell-to-cell movement of TGB1 and TGB2 and that TGB3 also blocks the movement of WT BNYVV when expressed ectopically at high levels from a separate replicon (3). In order to obtain a direct assessment of the effects of overexpression of TGB3 on WT BSMV infections, *C. amaranticolor* leaves were inoculated with infectious RNAα, -β, and -γ transcripts (20 μg) plus various amounts (0, 3, 6, or 9 μg) of RNAβ replicon transcripts. These replicons encode the CP and either the WT TGB3 sequence (β_{T3}) under the control of the *sgRNAβ1* promoter or a mutant (β_{T3mut}) $TGB3_{P105R,I108R}$ sequence that is unable to function in cell-to-cell movement (Fig. 7A). Numerous necrotic lesions were elicited on leaves inoculated with RNAα, -β, and -γ in the absence of β_{T3} (Fig. 7B). However, a dramatic reduction in the number of lesions occurred upon inoculation of mixtures containing 3 and 6 μg of $RNA\beta_{T3}$ transcripts, and addition of 9 μg of $RNA\beta_{T3}$ transcripts completely abolished lesion formation (Fig. 7C). In contrast, similar numbers of lesions were observed in *C. amaranticolor* coinoculated with RNAα, -β, -γ at all three concentrations of β_{T3mut} (Fig. 7D). Mock-inoculated leaves and controls inoculated with 6 μg of β_{T3} or β_{T3mut} alone failed to develop lesions as expected (Fig. 7B, C, and D). These results thus suggest strongly that appropriate levels of TGB3 expression are critical for BSMV movement and that the inhibitory effect requires TGB3-TGB2 binding interactions.

Both class I and class II TGB3 proteins are present in such low abundance that they are extremely difficult to detect in infected plants (9, 11, 29). Therefore, to provide an indirect evaluation of the expression the WT virus and the β_{T3} or β_{T3mut} TGB3 overexpression construct, total RNA was extracted from inoculated leaves, and RT-PCR was performed with two sets of primers. Together, these two primer pairs generated products from both the gRNAβ and TGB3 overexpression replicons. The forward primer (CP5′) was the same in both reactions and spanned the five N-terminal codons in the CP-encoding gene. In the first reaction, the reverse primer (TGB3 3′) was complementary to the seven C-terminal codons within the TGB3 sequence. This primer set was designed to generate a 1.2-kb product with a size that is specific to the TGB3 overexpression constructs. Additionally, this primer set could amplify an approximately 2.7-kb fragment from $RNA\beta_{wt}$ but the PCR conditions were designed to have a short extension time to prevent the generation of the larger product. The second primer set paired the CP5′ forward primer with a reverse primer (CP3′) in order to amplify the 0.6-kb CP product from β_{T3}, β_{T3mut}, and $RNA\beta_{wt}$ and to serve as a BSMV infection control (Fig. 7B, D, and F). In the WT BSMV positive control lacking the β_{T3} overexpression derivative, the 0.6-kb CP product was observed but the 1.2-kb product was absent. Neither PCR product was amplified from the mock-inoculated negative control (Fig. 7B). In plants inoculated with the TGB3 overexpression constructs, all of the leaves that developed necrotic lesions yielded RT-PCR fragments of the sizes expected for the CP alone (0.6 kb) and the CP-TGB3 derivative (1.2 kb) but products were not amplified from RNA extracted from leaves lacking lesions (Fig. 7C and D). These results indicate that the CP-TGB3 overexpression derivatives only replicated in the presence of the BSMV gRNAs, and they provide additional evidence that high levels of the WT TGB3 protein are detrimental to BSMV infection.

Separation of TGB expression compromises cell-to-cell movement. We have previously shown that expression of the BSMV TGB proteins is highly coordinated and depends on both transcriptional and translational controls (41). In WT BSMV, the TGB1 protein is translated from sgRNAβ1, which is relatively abundant, and the TGB2 and TGB3 proteins are expressed from low-abundance sgRNAβ2 (41). Translation of TGB2 is initiated by ribosomal assembly at the first sgRNAβ2 ORF, whereas TGB3 translation results from leaky ribosomal scanning to the second ORF. We have previously shown that this expression strategy results in TGB1/TGB2/TGB3 ratios of approximately 100:10:1 in BSMV-infected tissue (11) and in protoplasts (41).

In order to investigate the effects of the relative concentrations of the TGB proteins on cell-to-cell movement and the requirements for *cis* versus *trans* expression, we engineered genetic systems for BSMV in which overlapping TGB ORFs could be expressed individually from combinations of different gRNAs (Fig. 8A). The $\beta_{T1ssmut}$ derivative contains two site-specific mutations that interfere with virus cell-to-cell movement (22) and subcellular targeting of TGB2 (H.-S. Lim et al., unpublished data) plus a premature stop codon that truncates the TGB3 ORF at amino acid 72. In a second derivative ($\beta_{T1\Delta2,3}$), the overlapping TGB2/3 ORFs were deleted completely (Fig. 8A). Two constructs were also designed to permit *cis* expression of the TGB2 and -3 proteins. In the $\beta_{T2,3L}$ construct, a deletion from the NcoI to the SalI site was engineered to eliminate the expression of TGB1 while maintaining the TGB2 and -3 ORFs under the control of the *sgRNAβ2* promoter. The $\beta_{T2,3H}$ derivative was constructed to obtain higher levels of expression of TGB2 and TGB3 in *cis* by deleting the TGB1 ORF and inserting the TGB2 and TGB3 genes at the NcoI site that normally overlaps the TGB1 start codon. This manipulation placed the TGB2 and -3 ORFs directly under the control of the strong *sgRNAβ1* promoter (Fig. 8A). To evaluate the expression of greater amounts of the TGB2 and -3 proteins in *trans*, separate β_{T2} and β_{T3} gRNA derivatives were constructed in which the TGB2 or TGB3 ORF was placed under the control of the *sgRNAβ1* promoter.

When TGB2 and TGB3 were expressed in *trans* by inoculation of leaves with five component BSMV derivatives consisting of RNAα and -γ plus gRNAs $\beta_{T1ssmut}$, β_{T2}, and β_{T3} or gRNAs $\beta_{T1\Delta2,3}$, β_{T2}, and β_{T3}, local lesions failed to appear on *C. amaranticolor* (Fig. 8B), although some necrosis resulting from the inoculation procedure was observed. These results indicate that TGB proteins expressed individually from separate gRNAs were unable to function in cell-to-cell movement. However, with quadripartite inocula containing RNAα and -γ, plus the RNAβ derivatives $\beta_{T1ssmut}$ and $\beta_{T2,3L}$ or $\beta_{T1ssmut}$ and $\beta_{T2,3H}$, in which TGB2 and TGB3 are expressed in *cis*, leaves developed small lesions. In these leaves, the appearance of lesions was delayed by 5 or more days compared to those that received the inoculum containing $RNA\beta_{WT}$ (Fig. 8B). Comparisons of the inoculated leaves also reveal that higher levels of TGB2 and -3 expression from the $\beta_{T2,3H}$ derivative result in greater reductions in movement than the $\beta_{T2,3L}$ derivative. By 12 dpi, lesions were larger in leaves inoculated with combinations containing $\beta_{T1ssmut}$ and $\beta_{T2,3L}$ than in leaves inoculated

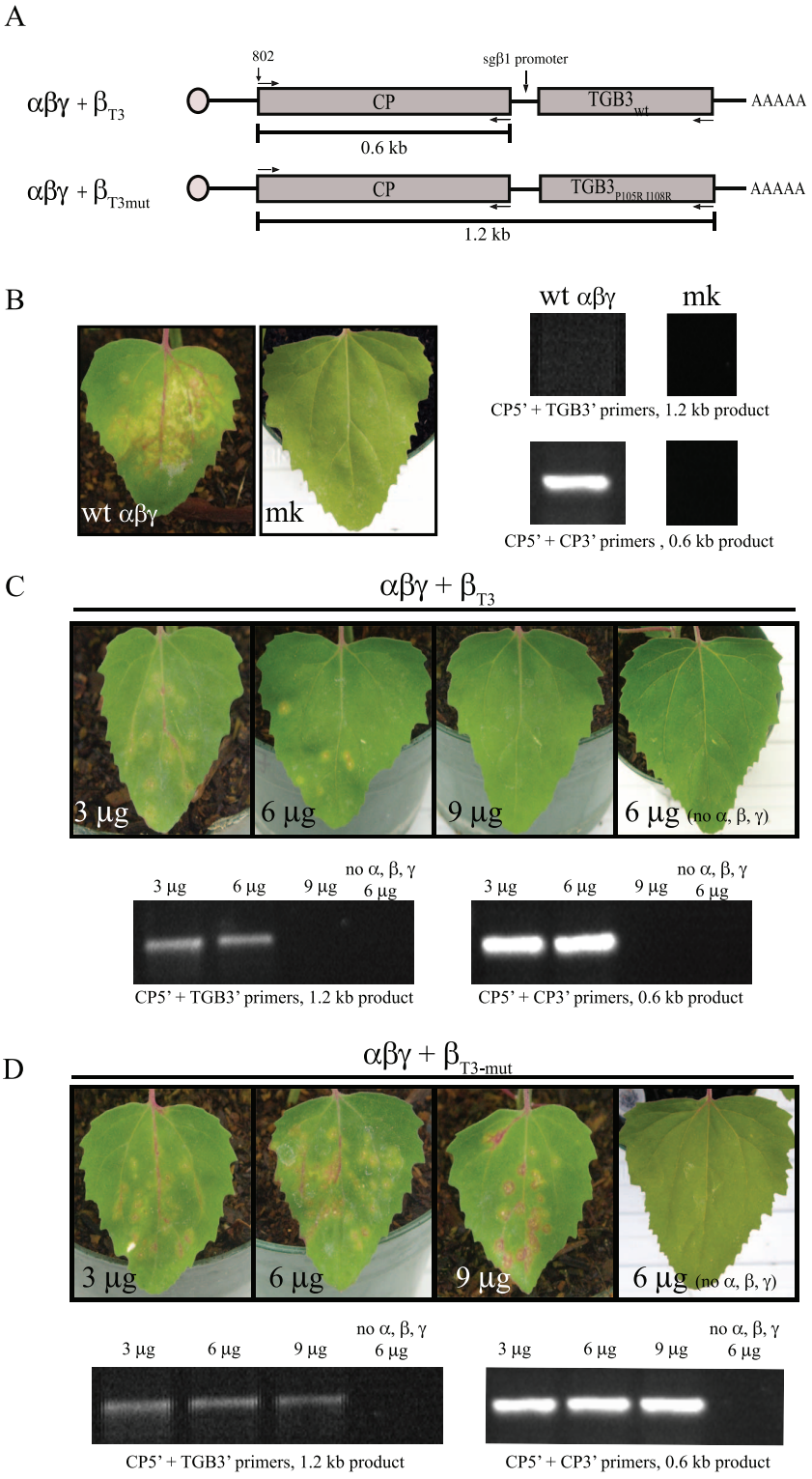

FIG. 7. Effects of overexpression of TGB3 on BSMV movement. (A) Depiction of RNAβ replicons designed for overexpression of $TGB3_{WT}$ (β_{T3}) or the $TGB3_{P105R;I108R}$ double mutant (β_{T3mut}). Overexpression of the TGB3 derivatives was accomplished by placing the ORF under the control of the *TGB1* promoter. The locations of primers used for RT-PCR are designated by black arrows above and below the boxes. (B) *C. amaranticolor* leaves were inoculated with 20 μg each of infectious RNAα, -β, and -γ transcripts or mock inoculated with buffer lacking RNA. Only leaves inoculated with RNAα, -β, and -γ developed lesions. RT-PCR amplifications with BSMV-specific primers are shown to the right of the leaves. (C) RNAα, -β, and -γ infectious transcripts plus different amounts of the $TGB3_{WT}$ overexpression replicon were inoculated into leaves. The three leaves on the left show progressive reductions in the numbers of lesions caused by coinoculations of RNAα, -β, and -γ with 3 μg, 6 μg, or 9 μg of the $TGB3_{WT}$ overexpression replicon, respectively. The control leaf on the right was inoculated with only the $TGB3_{WT}$ overexpression replicon and hence did not develop lesions. RT-PCR amplifications with specific primers are illustrated below the leaves. (D) Inoculations and PCR were carried out as for panel C, except that the inoculum contained the $TGB3_{P105R;I108R}$ overexpression replicon. Note that the 0.6-kb PCR product represents amplification from both the full-length RNAβ and RNAβ overexpression replicons. The 1.2-kb PCR product is generated from only the overexpression constructs.

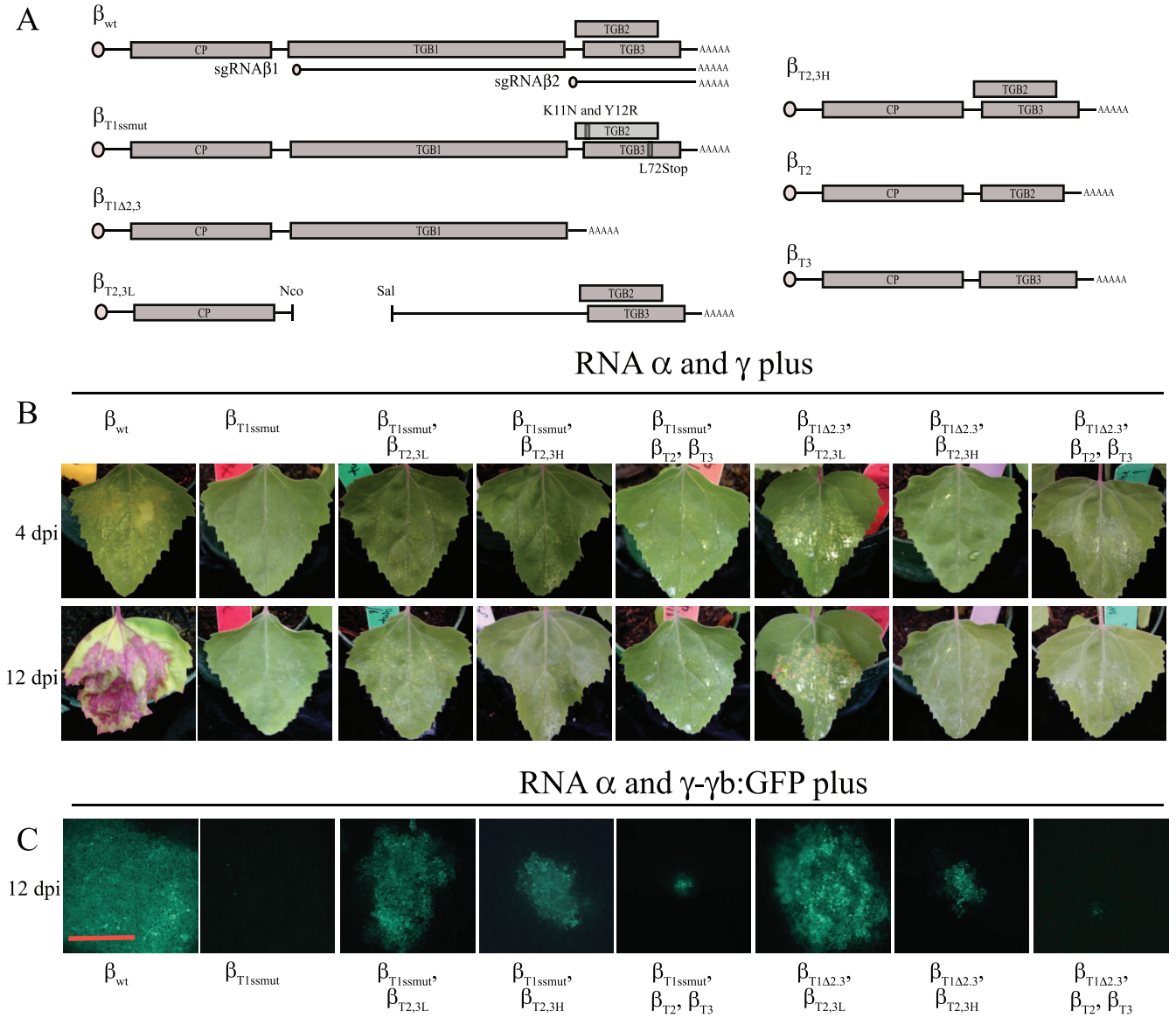

FIG. 8. Effects of *cis* and *trans* expression of the TGB2 and -3 proteins on infection. (A) RNAβ constructs designed for *cis* and *trans* expression of TGB2 and -3. Open circles represent the 5′ cap structures, and the internal poly(A) tract is designated at the 3′ end. Note that the 3′ 238-nt tRNA-like structure is not shown in these drawings. β_{WT} = WT RNAβ. The sgRNAβ1 and sgRNAβ2 mRNAs are illustrated as solid lines below β_{WT}; $\beta T1_{SSMUT}$ = RNAβ containing substitutions for residues at positions 11 and 12 in TGB2 that result in the production of a nonfunctional protein and a mutation in the TGB3 ORF that introduces a premature stop codon to yield a protein truncated at residue 72; $\beta_{T1\Delta2,3}$ = RNAβ with a 525-nt deletion of the TGB2/3 ORFs extending from the stop codon of TGB1 to the poly(A) tract; $\beta_{T2,3L}$ = RNAβ with a deletion in the TGB1 ORF that maintains expression of the sgRNAβ2 under the control of the *sgRNAβ2* promoter to facilitate low-level expression of the TGB2 and -3 proteins; $\beta_{T2,3H}$ = RNAβ with a deletion of the TGB1 ORF that permits high-level *cis* expression of TGB2 and -3 under the control of the *sgRNAβ1* promoter; β_{T2} = RNAβ containing deletions of the TGB1 and the TGB3 ORFs to facilitate high-level expression of TGB2 under the control of the *sgRNAβ1* promoter; β_{T3} = RNAβ containing deletions of the TGB1 and TGB2 ORFs to facilitate high-level expression of TGB3 under the control of the *sgRNAβ1* promoter. (B) Local lesion development in *C. amaranticolor* leaves inoculated with RNAα and -γ plus β_{WT} or different combinations of the *cis* and *trans* TGB protein expression derivatives. Leaves were photographed at 4 and 12 dpi. (C) Fluorescence in *N. benthamiana* leaves at 12 dpi after inoculation with RNAα and RNAγ-GFP plus the RNAβ derivatives designated below the leaves.

with the $\beta_{T1ssmut}$ and $\beta_{T2,3H}$ derivatives (Fig. 8B). Furthermore, lesions were not evident upon coinoculation of $\beta_{T1\Delta2,3}$ and $\beta_{T2,3H}$, but when $\beta_{T1\Delta2,3}$ was paired with $\beta_{T2,3L}$, the timing of lesion appearance was similar to that elicited by β_{wt}, although radial spread of the lesions was reduced substantially (Fig. 8B). Total RNA was extracted from inoculated leaves at 10 dpi and subjected to Northern blot analysis. In these experiments, viral RNA was detected only in samples of leaves that were developing lesions (data not shown). These leaves included the β_{wt} positive control and the gRNAβ combinations $\beta_{T1ssmut}$ and $\beta_{T2,3L}$, $\beta_{T1ssmut}$ and $\beta_{T2,3H}$, and $\beta_{T1\Delta2,3}$ and $\beta_{T2,3L}$. Furthermore, the intensity of the signal amplification reflected the timing and severity of symptom development observed in the inoculated leaves, with the β_{wt} and $\beta_{T1\Delta2,3}$

samples displaying a much stronger signal than the $\beta_{T1ssmut}$ samples (data not shown).

To provide a more sensitive nonlesion assay to permit visualization of virus movement, *N. benthamiana* plants were coinoculated with the same combinations of RNAβ derivatives described above plus a WT RNAα transcript and an RNAγ derivative encoding a γb-GFP fusion protein (Fig. 8C). Fluorescence of different combinations of the RNAβ derivatives at 12 dpi demonstrated that the extent of virus spread varied substantially in inoculated leaves, depending on the promoter used for expression of TGB2 and TGB3 and the inoculum composition. Inocula containing $RNA\beta_{wt}$ elicited the largest infection foci (>100 μm), whereas the $\beta_{T2,3H}$ and $\beta_{T2,3L}$ combinations expressing TGB2 and -3 in *cis* under the control of the *sgRNAβ1* or *sgRNAβ2* promoter, respectively, developed smaller foci (estimated to range from 25 to 75 μm diameter). Moreover, fluorescent foci observed when inocula contained $\beta_{T2,3H}$, in which TGB2 and TGB3 are expressed under the control of the *sgRNAβ1* promoter, were substantially smaller than those associated with $\beta_{T2,3L}$-inoculated leaves. When TGB2 and TGB3 were expressed in *trans* from β_{T2} and β_{T3} in combination with $\beta_{T1\Delta2,3}$, multicell foci did not appear; however, inocula containing $\beta_{T1ssmut}$, β_{T2}, and β_{T3} developed a few foci that appeared to be three to four cells in diameter. In contrast $\beta_{T1\Delta2,3}$, β_{T2}, and β_{T3} failed to elicit discernible fluorescent foci extending beyond single cells (Fig. 8C). These results thus demonstrate that *cis* expression of the TGB2 and -3 proteins is required for effective cell-to-cell movement and show that elevated levels of TGB2 and -3 expression from the *sgRNAβ1* promoter in the $\beta_{T2,3H}$ mutant are less effective at facilitating movement than the lower levels of TGB2 and TGB3 expressed from the *sgRNAβ2* promoter functioning in the $\beta_{T2,3L}$ mutant.

In an additional series of experiments, barley plants were inoculated with the same inoculum combinations used for *N. benthamiana*. However, only virus containing RNAα and -γ plus $RNA\beta_{wt}$ developed symptoms, and fluorescent foci were not detected (data not shown). These results are similar to those previously obtained by Lawrence and Jackson (22) and reiterate the limited usefulness of barley and other cereals as hosts for the assessment of BSMV cell-to-cell movement.

DISCUSSION

Several lines of genetic and biochemical evidence presented in this study indicate that the TGB proteins participate in complex interactions that are required for BSMV cell-to-cell movement. These include characterization of a TGB1 RNP complex that is apparently analogous to the RNP first identified by Brakke et al. (7). In other experiments, we obtained evidence for homologous TGB1 interactions and heterologous binding of TGB1 to TGB3 and TGB2 to TGB3. Site-specific requirements for these interactions have been identified, and mutations that disrupt the interactions have been shown to interfere with the cell-to-cell movement of BSMV. We also have shown that the ratios of TGB protein expression and the contexts in which they are expressed have substantial effects on the rates of BSMV movement. In particular, elevated expression of the normally low-abundance TGB3 protein interferes with movement but overexpression of a site-specific TGB3 mutant that interferes with its ability to bind TGB2 fails to affect movement. These results extend previous studies and provide a model of BSMV movement that requires RNP complexes mediated by homologous interactions of TGB1 during viral RNA binding, direct associations of TGB1 and TGB3, and formation of TGB2 and TGB3 interactions to target the localization of the RNPs through PD into adjacent cells.

Our experiments show that the RNP recovered from BSMV-infected plants is a salt-stable complex composed of the TGB1 protein and gRNAs and sgRNAs expressed during infection. On the basis of previous genetic studies showing that TGB1 is required for cell-to-cell movement and that the CP is dispensable for infection (22, 30), we propose that the RNP is the primary determinant for transport of BSMV RNAs during local and systemic virus invasion. Moreover, the heterogeneous sedimentation profile of the RNP suggests that plus-sense gRNAs and sgRNAs are the major components of the RNP and that TGB1 functions directly to bind the individual BSMV gRNAs and sgRNAs in planta. Because the BSMV TGB1 protein binds to dsRNAs in vitro, we hypothesized previously that dsRNA replication complexes might participate in cell-to-cell movement (10), but the absence of minus-strand RNAs in the RNP does not support this model and instead implicates plus-sense viral RNAs in local and systemic transport throughout the plant.

Physical interactions of the hordeivirus- and potexvirus-like TGB1 proteins are not well understood, but both classes of TGB1 proteins contain a conserved helicase domain related to the superfamily I helicases found in the replicase subunits of alpha viruses (29). Among other activities, helicases within this class often function in protein-protein binding (14), and a considerable body of evidence suggests that conserved residues within the helicase domain are critical for biological functions of the TGB1 proteins (29). With BSMV, the strong cooperative activity observed in our earlier RNA binding experiments suggests that TGB1 participates in homologous interactions (10), and recovery of the TGB1 RNP complex supports this notion. In addition, site-specific amino acid substitutions introduced into the six conserved helicase motifs of TGB1 abrogate BSMV cell-to-cell movement, interfere with several biochemical functions, and disrupt targeting of the TGB1 protein to the PD of infected cells (21). Therefore, it is plausible that self-interactions of TGB1 mediated by the helicase motif are required for some of these activities.

In order to investigate BSMV TGB1 binding in more detail, we conducted yeast two-hybrid and affinity chromatography assays to assess homologous and heterologous interactions. We were unable to detect BSMV TGB1 binding by using yeast two-hybrid analyses (Table 1), but BSMV TGB1 interactions were revealed by the use of experimental approaches differing from those used previously with potato mop-top virus (PMTV), PSLV, and PVX (9, 23, 34). We first obtained direct evidence for in vivo TGB1 binding by chemical cross-linking experiments. Although the cross-linking experiments do not distinguish homologous TGB1 binding from heterologous interactions with other viral and/or host components, a series of affinity chromatography experiments did verify homologous BSMV TGB1 binding. Moreover, mutagenesis of conserved amino acids within the full-length BSMV TGB1 protein extended the PSLV results by implicating amino acid residues

259, 339, and 340 within the two N-terminal helicase motifs as being critical for the TGB1 homologous interactions and demonstrated that substitution of conserved residues within two C-terminal motifs does not disrupt TGB1 interactions. We have also shown previously that incorporation of site-specific amino acid substitutions within each of the helicase motifs disrupts TGB1 localization to PD (21), and more recently, we have determined the effects of these and other mutations on the sequestration of TGB1 at various subcellular sites (Lim et al., unpublished).

Direct evidence implicating homologous interactions of a hordeivirus-like TGB1 protein was first obtained for PMTV by use of yeast two-hybrid and immunoblot overlay assays (9). More recent findings have also suggested that PVX and PSLV TGB1 proteins are capable of forming homologous associations (23). In the latter experiments, the full-length PVX 25-kDA and PSLV 63-kDa TGB1 proteins produced by in vitro translation both migrated as single bands in SDS-polyacrylamide gels. In addition, truncation mutants containing N-terminal helicase motifs I, II, and III formed SDS-resistant forms migrated as dimers in polyacrylamide gels, but the motifs were not analyzed to evaluate the requirements for the interactions. Our results have extended this study, and we have identified amino acid residues in the first two motifs that are critical for the homologous interactions of the BSMV TGB1 protein. Additional support for homologous binding of PVX TGB1 has also been obtained very recently by use of yeast two-hybrid experiments (34). In toto, these results suggest that TGB1 self-interactions are essential for the functional activities of both hordeivirus- and potexvirus-like TGB1 proteins.

A number of studies have suggested that TGB3 has a critical role in targeting hordeivirus-like TGB1 proteins to the PD or to peripheral vesicles around the cell wall (25, 29). To explore the mechanisms whereby these activities might be carried out, we initiated a series of GST affinity chromatography experiments to detect heterologous interactions between the TGB1 and TGB3 proteins recovered from yeast. These experiments clearly revealed TGB1-TGB3 binding, and they differ from the negative findings obtained with PMTV (9) and PVX (34). However, we were not able to detect TGB1 and TGB2 interactions by using either affinity chromatography or yeast two-hybrid analyses, nor were we able to identify the homologous TGB2 and TGB3 interactions reported previously with PMTV (9). Nevertheless, our findings are compatible with the view that direct TGB1-TGB3 interactions function in the subcellular transport of TGB1 RNP complexes and in BSMV cell-to-cell movement processes.

To obtain more information about TGB2-TGB3 interactions, we investigated GST affinity chromatography and yeast two-hybrid approaches. The yeast two-hybrid results permitted the construction of a series of site-specific amino acid substitutions within conserved regions of the hordeivirus TGB2 and TGB3 proteins. Among these mutants, a $TGB2_{G40R}$ substitution in the hydrophilic region of the protein failed to interact with TGB3. Similar site-specific mutations that disrupt heterologous TGB2-TGB3 binding mapped to $TGB3_{I108R}$ within the cytoplasmic domain. These results suggest that at least two amino acids that affect binding interactions reside outside of the hydrophobic transmembrane domains.

The biological context of the mutations that interfere with TGB2-TGB3 interactions was investigated by incorporating the mutations individually into RNAβ and conducting infectivity experiments with *N. benthamiana* and *C. amaranticolor*. The results clearly showed that both mutations interfered with detectable cell-to-cell movement, thus providing evidence indicating that TGB2-TGB3 binding interactions are important for virus transport. Moreover, expression of TGB3 from a replicon designed for high-level expression revealed that elevated amounts of WT TGB3 interfered with cell-to-cell movement but that overexpression of TGB3 mutants that are unable to interact with TGB2 did not affect movement. These results thus demonstrate that competition effects arising from TGB3 overexpression can interfere with BSMV cell-to-cell movement and provide a model suggesting that TGB2-TGB3 protein-protein interactions are required for these effects. This model clearly differs from the proposal of Lauber et al. (20) that inhibitory effects due to elevated expression of BNYVV TGB3 are an indirect consequence of changes in subcellular membrane architecture, rather than the result of altered TGB3 interactions.

We also investigated the *cis* and *trans* interactions of BSMV by expressing the TGB proteins from multiple RNAβ derivatives. The results of these experiments demonstrate that the TGB can be separated to generate quadripartite virus derivatives with varied abilities to move from cell to cell in inoculated leaves. However, comparisons of different quadripartite derivatives with the WT tripartite virus clearly shows that the most efficient cell-to-cell movement in *C. amaranticolor* and *N. benthamiana* occurs with WT BSMV and that movement beyond a few cells depends on the expression of TGB2 and TGB3 from the same mRNA. In the quadripartite virus, when a modified gRNAβ that cannot express TGB2 and -3 was coinoculated with a second gRNAβ designed to express low levels of TGB2 and -3 from the *sgRNAβ2* promoter, cell-to-cell movement was compromised but not eliminated completely. Moreover, with a different quadripartite virus designed for higher levels of expression of the TGB2 and TGB3 proteins under the control of the *sgRNAβ1* promoter, cell-to-cell movement was compromised to a greater extent. Therefore, our collective results indicate that the context in which the TGB proteins are expressed has profound effects on movement.

In sum, the results of the present study are compatible with a model in which the TGB1 protein forms nucleoprotein complexes with BSMV gRNAs and sgRNAs. Detection of interactions between TGB1 and TGB3 suggests that TGB3 may interact with the TGB1 RNP complexes to help mediate PDl localization and cell-to-cell movement. Although we were unable to detect TGB3 in the complexes, it should be noted that TGB3 is present in extremely low abundance in infected cells. The interactions of TGB2 and TGB3 also support a requirement for direct TGB interactions during movement, as suggested in our previous studies (21, 22). In addition, our results have direct implications for subcellular targeting of the hordeivirus-like TGB proteins, and our future research will focus on cytological analyses to evaluate their movement mechanisms in more detail.

ACKNOWLEDGMENTS

This research was supported by United States Department of Agriculture competitive grants 2005:35319-15307 and 2006:35319-16552.

REFERENCES

1. **Bayne, E. H., D. V. Rakitina, S. Y. Morozov, and D. C. Baulcombe.** 2005. Cell-to-cell movement of potato potexvirus X is dependent on suppression of RNA silencing. Plant J. **44:**471–482.
2. **Becker, D. M., J. D. Fikes, and L. Guarente.** 1991. A cDNA encoding a human CCAAT-binding protein cloned by functional complementation in yeast. Proc. Natl. Acad. Sci. USA **88:**1968–1972.
3. **Bleykasten-Grosshans, C., H. Guilley, S. Bouzoubaa, K. E. Richards, and G. Jonard.** 1997. Independent expression of the first two triple gene block proteins of beet necrotic yellow vein virus complements virus defective in the corresponding gene but expression of the third protein inhibits viral cell-to-cell movement. Mol. Plant-Microbe Interact. **10:**240–246.
4. **Boevink, P., and K. J. Oparka.** 2005. Virus-host interactions during movement processes. Plant Physiol. **138:**1815–1821.
5. **Bragg, J. N., and A. O. Jackson.** 2004. The C-terminal region of the barley stripe mosaic virus γb protein participates in homologous interactions and is required for suppression of RNA silencing. Mol. Plant Pathol. **5:**465–481.
6. **Bragg, J. N., H. S. Lim, and A. O. Jackson.** 2008. Hordeiviruses. *In* B. Mahy and M. van Regenmortel (ed.), Encyclopedia of virology, 3rd ed., in press. Elsevier Ltd., Oxford, United Kingdom.
7. **Brakke, M. K., E. M. Ball, and W. G. Langenberg.** 1988. A non-capsid protein associated with unencapsidated virus RNA in barley infected with barley stripe mosaic virus. J. Gen. Virol. **69:**481–491.
8. **Chapman, S., G. Hills, J. Watts, and D. Baulcombe.** 1992. Mutational analysis of the coat protein gene of potato virus X: effects on virion morphology and viral pathogenicity. Virology **191:**223–230.
9. **Cowan, G. H., F. Lioliopoulou, A. Ziegle, and L. Torrance.** 2002. Subcellular localisation, protein interactions, and RNA binding of potato mop-top virus triple gene block proteins. Virology **298:**106–115.
10. **Donald, R. G. K., D. M. Lawrence, and A. O. Jackson.** 1997. The barley stripe mosaic virus 58-kilodalton βb protein is a multifunctional RNA binding protein. J. Virol. **71:**1538–1546.
11. **Donald, R. G. K., H. Zhou, and A. O. Jackson.** 1993. Serological analysis of barley stripe mosaic virus-encoded proteins in infected barley. Virology **195:**659–668.
12. **Fancy, D. A., K. Melcher, S. A. Johnston, and T. Kodadek.** 1996. New chemistry for the study of multiprotein complexes: the six-histidine tag as a receptor for a protein crosslinking reagent. Chem. Biol. **3:**551–559.
13. **Goodin, M. M., J. Austin, R. Tobias, M. Fujita, C. Morales, and A. O. Jackson.** 2001. Interactions and nuclear import of the N and P proteins of sonchus yellow net virus, a plant nucleorhabdovirus. J. Virol. **75:**9393–9406.
14. **Gorbalenya, A. E., and E. V. Koonin.** 1993. Helicases: amino acid sequence comparisons and structure-function relationships. Curr. Opin. Struct. Biol. **3:**419–429.
15. **Heinlein, M., and B. L. Epel.** 2004. Macromolecular transport and signaling through plasmodesmata. Int. Rev. Cytol. **235:**93–164.
16. **James, P., J. Halladay, and E. A. Craig.** 1996. Genomic libraries and a host strain designed for highly efficient two-hybrid selection in yeast. Genetics **144:**1425–1436.
17. **Johnson, J. A., J. N. Bragg, D. M. Lawrence, and A. O. Jackson.** 2003. Sequence elements controlling expression of barley stripe mosaic virus subgenomic RNAs in vivo. Virology **313:**66–80.
18. **Kalinina, N. O., D. V. Rakitina, A. G. Solovyev, J. Schiemann, and S. Y. Morozov.** 2002. RNA helicase activity of the plant virus movement proteins encoded by the first gene of the triple gene block. Virology **296:**321–329.
19. **Karpova, O. V., O. V. Zayakina, M. V. Arkhipenko, E. V. Sheval, O. I. Kiselyova, V. Y. Poljakov, I. V. Yaminsky, N. P. Rodionova, and J. G. Atabekov.** 2006. Potato virus X RNA-mediated assembly of single-tailed ternary 'coat protein-RNA-movement protein' complexes. J. Gen. Virol. **87:**2731–2740.
20. **Lauber, E., G. Jonard, K. E. Richards, and H. Guilley.** 2005. Nonregulated expression of TGBp3 of hordei-like viruses but not of potex-like viruses inhibits beet necrotic yellow vein virus cell-to-cell movement. Arch. Virol. **17:**1459–1467.
21. **Lawrence, D. M., and A. O. Jackson.** 2001. Interactions of the TGB1 protein during cell-to-cell movement of *Barley stripe mosaic virus*. J. Virol. **75:**8712–8723.
22. **Lawrence, D. M., and A. O. Jackson.** 2001. Requirements for cell-to-cell movement of barley stripe mosaic virus in monocot and dicot hosts. Mol. Plant Pathol. **2:**65–75.
23. **Leshchiner, A. D., A. G. Solovyev, S. Y. Morozov, and N. O. Kalinina.** 2006. A minimal region in the NTPase/helicase domain of the TGBp1 plant virus movement protein is responsible for ATPase activity and cooperative RNA binding. J. Gen. Virol. **87:**3087–3095.
24. **Li, F., and S. Ding.** 2006. Virus counterdefense: diverse strategies for evading the RNA silencing immunity. Annu. Rev. Microbiol. **60:**503–531.
25. **Lucas, W. J.** 2006. Plant viral movement proteins: agents for cell-to-cell trafficking of viral genomes. Virology **344:**169–184.
26. **MacDiarmid, R.** 2005. RNA silencing in productive virus infections. Annu. Rev. Phytopathol. **43:**523–544.
27. **Melcher, U.** 2000. The '30K' superfamily of viral movement proteins. J. Gen. Virol. **81:**257–266.
28. **Miller, C. A., III, M. A. Martinat, and L. E. Hyman.** 1998. Assessment of aryl hydrocarbon receptor complex interactions using pBEVY plasmids: expression vectors with bi-directional promoters for use in *Saccharomyces cerevisiae*. Nucleic Acids Res. **26:**3577–3583.
29. **Morozov, S. Y., and A. G. Solovyev.** 2003. Triple gene block: modular design of a multifunctional machine for plant virus movement. J. Gen. Virol. **84:**1351–1366.
30. **Petty, I. T. D., and A. O. Jackson.** 1990. Mutational analysis of barley stripe mosaic virus RNAβ. Virology **179:**712–718.
31. **Petty, I. T. D., R. French, R. W. Jones, and A. O. Jackson.** 1990. Identification of barley stripe mosaic virus genes involved in viral RNA replication and systemic movement. EMBO J. **9:**3453–3457.
32. **Petty, I. T. D., B. G. Hunter, and A. O. Jackson.** 1988. A novel strategy for one-step cloning of full-length cDNA and its application to the genome of barley stripe mosaic virus. Gene **74:**423–432.
33. **Petty, I. T., B. G. Hunter, N. Wei, and A. O. Jackson.** 1989. Infectious barley stripe mosaic virus RNA transcribed in vitro from full-length genomic cDNA clones. Virology **171:**342–349.
34. **Samuels, T. D., H. J. Ju, C. M. Ye, C. M. Motes, E. B. Blancaflor, and J. Verchot-Lubicz.** 2007. Subcellular targeting and interactions among the potato virus X TGB proteins. Virology **367:**375–389.
35. **Verchot, J., S. M. Angell, and D. C. Baulcombe.** 1998. In vivo translation of the triple gene block of potato virus X requires two subgenomic mRNAs. J. Virol. **72:**8316–8320.
36. **Verchot-Lubicz, J.** 2005. A new cell-to-cell transport model for potexviruses. Mol. Plant-Microbe Interact. **18:**283–290.
37. **Verchot-Lubicz, J., C. M. Ye, and D. Bamunusinghe.** 2007. Molecular biology of potexviruses: recent advances. J. Gen. Virol. **88:**1643–1655.
38. **Waigmann, E., S. Ueki, K. Trutnyeva, and V. Citovsky.** 2004. The ins and outs of nondestructive cell-to-cell and systemic movement of plant viruses. Crit. Rev. Plant Sci. **23:**195–250.
39. **Wong, S. M., K. C. Lee, H. H. Yu, and W. F. Leong.** 1998. Phylogenetic analysis of triple gene block viruses based on the TGB 1 homolog gene indicates a convergent evolution. Virus Genes **16:**295–302.
40. **Wurch, T., F. Lestienne, and P. Pauwels.** 1998. A modified overlap extension PCR method to create chimeric genes in the absence of restriction enzymes. Biotechnol. Tech. **12:**653–657.
41. **Zhou, H., and A. O. Jackson.** 1996. Expression of the barley stripe mosaic virus RNA β "triple gene block". Virology **216:**367–379.